ChemComm

HIGHLIGHT

View Article Online
View Journal | View Issue

Check for updates

Cite this: *Chem. Commun.*, 2025, **61**, 4881

Polyoxometalates for the catalytic reduction of nitrogen oxide and its derivatives: from novel structures to functional applications

Yuan Jiang,† Chun-Jun Chen,† Ke Li,† Li-Ping Cui and Jia-Jia Chen *

Nitrogen oxide and its derivatives, including nitroaromatic hydrocarbons and various other nitro compounds, are commonly used in industrial applications such as synthesizing drugs, dyes, pesticides, and explosives. However, these compounds are also highly toxic to the environment. Their long-term accumulation can significantly affect air and water quality and disrupt ecosystems. Thus, efficiently converting these harmful compounds into more valuable products through catalytic processes is an urgent challenge in chemical catalysis. In this regard, polyoxometalates (POMs) have emerged as promising inorganic molecular catalysts for the reduction of nitrogen oxide and its derivatives. Their unique structure, excellent redox properties, and versatile catalytic abilities contribute to their effectiveness. This review provides an overview of recent advancements in the POM-catalyzed reduction of nitrogen oxide and its derivatives, focusing on reducing nitroaromatic hydrocarbons and nitrogen oxides. Additionally, we discuss the reaction mechanisms involved in the catalytic process, explore the potential of POMs' structural features for the rational design and optimization of catalytic performance, and highlight future directions for developing POM-based catalysts.

Received 5th February 2025,
Accepted 27th February 2025

DOI: 10.1039/d5cc00632e

rsc.li/chemcomm

Open Access Article. Published on 28 February 2025. Downloaded on 2026-01-28 12:39:06 PM.
This article is licensed under a Creative Commons Attribution-NonCommercial 3.0 Unported Licence.

State Key Laboratory for Physical Chemistry of Solid Surfaces, Innovation Laboratory for Sciences and Technologies of Energy Material of Fujian Province (IKKEM), Collaborative Innovation Center of Chemistry for Energy Materials (iChem), Engineering Research Center of Electrochemical Technologies of Ministry of Education, Department of Chemistry, College of Chemistry and Chemical Engineering, Xiamen University, Xiamen, Fujian, 361005, China.
E-mail: jiajia.chen@xmu.edu.cn
† These authors contributed equally to this work.

1. Introduction

Catalytic reduction of nitrogen oxide and its derivatives is paramount in academic research and environmental governance, with widespread use in industrial production.[1–4] Nitrogen oxide and its derivatives are primarily by-products of industrial activities and fuel combustion, posing significant environmental hazards. The conversion of these toxic substances into value-

The first one on the left in the second row in this group photo is Dr Jia-Jia Chen

Prof. Dr Jia-Jia Chen received his BSc and PhD from the Department of Chemistry at Xiamen University in 2009 and 2014, respectively. Then he carried out his postdoctoral research with Prof. Leroy Cronin at the University of Glasgow (2015–2018). He started his independent research in December of 2018 and built his own research team at Xiamen University. His group research interests mainly include the following two aspects: (1) the structural evolution and self-assembly of redox-active materials with multi-electron redox ability. Our group can build operand spectroscopy techniques to reveal the self-assembly behaviors of clusters with multi-electron redox ability. This will, in turn, help us design interesting materials rationally. (2) Functional electrolytes and the related physical electrochemistry in soluble and solid states. Metal–oxo clusters can exist in aqueous, nonaqueous, and solid-state electrolytes/polymer electrolytes, which will play important roles in solar/thermal/electrical-driven energy storage and conversion systems.

Open Access Article. Published on 28 February 2025. Downloaded on 2026-01-28 12:39:06 PM. This article is licensed under a Creative Commons Attribution-NonCommercial 3.0 Unported Licence.

added products through catalytic reduction offers substantial economic and environmental benefits. For example, functionalized anilines, mainly synthesized by catalytic hydrogenation of nitroaromatic compounds, are widely applied in various industries, including agrochemicals, dyes, fragrances and pharmaceuticals.[5,6] Meanwhile, with the growing intensity of human activities, the emission of nitrogen oxides (NO_x) has become an increasing environmental concern. These pollutants are released into the environment in substantial quantities in both gaseous (*e.g.*, NO, N_2O)[7] and ionic (*e.g.*, NO_3^-; NO_2^-)[8] forms, contributing to the eutrophication of water bodies and an imbalance in the global nitrogen cycle. The catalytic reduction of nitrogen oxides to ammonia presents a highly promising solution for restoring the nitrogen cycle. Ammonia serves as a critical feedstock for the manufacture of fertilizers, nitric acid, and explosives, and emerges as a promising green energy carrier for hydrogen storage in fuel cells.[9,10] Therefore, the catalytic reduction of nitrogen oxide and its derivatives offers a dual benefit: it can serve as an effective pollutant mitigation strategy while also providing a significant pathway for the synthesis of valuable chemical raw materials.[11]

However, the catalytic reduction of nitrogen oxide and its derivatives is not straightforward, as it typically involves the complex transfer of multiple electrons and protons (*e.g.*, NO_3RR: $NO_3^- + 9H^+ + 8e^- \rightarrow NH_3 + 3H_2O$, Ph-$NO_2$ + $6e^-$ + $6H^+ \rightarrow$ Ph-NH_2), resulting in various reaction intermediates and by-products.[12,13] Moreover, when treating industrial wastewater containing nitrates, certain substances can cause catalyst poisoning, thereby affecting the stability and efficiency of the catalyst. Therefore, it is crucial to focus on developing catalysts that exhibit efficiency, high selectivity, and stability.[14,15]

Polyoxometalates (POMs) are a class of metal–oxide cluster compounds composed of high-valent transition metals, such as Mo, W, V, Nb, and Ta, coordinated with oxygen atoms.[16] POMs exhibit diverse structures and unique optoelectronic properties, leading to their widespread applications in pharmaceuticals,[16] catalysis,[17] materials science[18] and energy.[19] In recent years, the use of POMs in the catalytic reduction of nitrogen oxide and its derivatives has garnered increasing attention.[20,21]

On the one hand, POMs have well-defined molecular structures and are considered the ideal model for studying single metal atom anchoring, which aids in understanding catalytic mechanisms and structure–activity relationships.[22,23] On the other hand, the tunable composition of POMs allows for precise design at both molecular and atomic scales, facilitating adjustments in characteristics such as acidity, redox potential, and stability. This enables the customized synthesis of high-performance catalysts.[24,25] In addition, POMs exhibit a synergistic effect when combined with other materials, such as transition metal catalysts and semiconductor materials, thereby facilitating multifunctional catalytic processes.[16,26] The interaction between POMs and their carriers allows for the customized assembly and construction of multidimensional structures, which shows great promise for the catalytic reduction of nitrogen oxide and its derivatives. Furthermore, while noble metal catalysts often degrade under harsh conditions,[27] POM-based catalysts can be enhanced for improved thermal and chemical stability through modifications in metal composition, ligand structure, and functional group substitution. The structural tunability of POMs enables targeted optimization of reaction pathways while minimizing side reactions.[28–30] Additionally, their earth-abundant components provide significant economic advantages over precious metals.[31] Moreover, POMs can act as unique "electron sponges",[32,33] enabling them to manage electron transfer processes during catalytic reactions efficiently. These collective attributes position POMs as promising candidates for scalable industrial applications in sustainable catalytic systems.

In this review, strategies for modulating the properties of the POM catalysts and their application in the catalytic reduction of nitro derivatives are summarized and discussed. It begins by introducing the fundamental properties of POMs and outlining their advantages in catalysis. Next, various modulation techniques and their impact on catalytic performance are explored, with highlights of examples of POM applications in reducing nitrogen oxide and its derivatives, such as nitroaromatics and nitrogen oxides. In the final sections, we focus on enhancing the performance and selectivity through rational catalyst design, advanced characterization techniques, and modulation approaches. Additionally, we emphasize the development of low-energy, high-efficiency catalytic systems that align with the principles of green catalysis, which are expected to enhance the practical application of POM-based catalysts in industrial processes.

2. Strategies for the regulation of POM-based catalysts

Polyoxometalates (POMs) are metal–oxo clusters composed of transition metal ions interconnected by oxygen atoms. The essential building blocks of these structures are metal oxide polyhedra represented as $\{MO_x\}$ (where x can be 5 or 6). In these polyhedra, M typically stands for early transition metals (such as W, Mo, V, Nb, Ta, *etc.*), which are often in a highly oxidized state. Furthermore, these metal centers can be partially substituted by other metals.[34] POMs can be classified in various ways, but they are most commonly divided into two primary categories based on their constituent elements: isopoly acids and heteropoly acids. In isopoly acids, only one central metal atom is bonded to oxygen; examples include molybdate ($Mo_6O_{19}^{2-}$) and tungstate ($W_{12}O_{39}^{2-}$). In contrast, heteropoly acids have a more complex structure, incorporating additional heteroatoms alongside the central metal and oxygen atoms. This inclusion of heteroatoms imparts distinctive chemical properties, as demonstrated by compounds such as phosphomolybdate ($H_3PW_{12}O_{40}$) and silicotungstate ($H_4SiW_{12}O_{40}$). Depending on the specific structure of the anion, POMs can be further subdivided into various families, including Keggin, Dawson, Anderson, and Waugh, each characterized by unique structural features.[35]

In solution, heteropoly acids (HPAs) function as super-strong Brønsted acids, being even more acidic than traditional

 This journal is © The Royal Society of Chemistry 2025

Open Access Article. Published on 28 February 2025. Downloaded on 2026-01-28 12:39:06 PM.
This article is licensed under a Creative Commons Attribution-NonCommercial 3.0 Unported Licence.

inorganic acids like HCl, H_2SO_4, and HNO_3. Solid HPAs are also more acidic than typical solid acids such as H_2SO_4/SiO_2, H_3PO_4/SiO_2, and SiO_2/Al_2O_3.[36] Additionally, POMs exhibit basic properties due to the abundance of bridging and terminal oxygen atoms on their polyanion surfaces, which allow them to donate electrons to electron acceptors. Conversely, the metal ions within the POM structure possess empty orbitals, enabling them to accept electrons, which allows POMs to function as Lewis acids as well.[37] This ability to both donate and accept electrons demonstrates that POMs possess excellent redox properties under varying conditions. Consequently, POMs can act as Lewis acids, Lewis bases, ligands, or catalysts, depending on the specific environment and their oxygen reduction properties.[38] As a class of highly diverse and structurally tunable functional materials, POMs exhibit significant potential for applications in materials science and catalysis. Their unique structural characteristics allow for precise regulation of their properties by manipulating factors such as the type of central metal, the nature and quantity of heteroatoms, and the optimization of synthesis conditions (*e.g.*, temperature, pH, and reactant concentration).[39] This tunability makes POMs suitable for a wide range of catalytic applications under various reaction conditions.

For example, as illustrated in Fig. 1, the saturated Keggin structure can undergo the controlled removal of one, two, or three metal–oxygen units by adjusting the pH or ionic strength of the solution. This results in lacunary Keggin POMs, such as mono-lacunary (1 : 11), di-lacunary (1 : 10), and tri-lacunary (1 : 9) POMs.[39] These lacunary POMs, which still possess numerous oxygen ligand sites, can engage in coordination reactions with transition metal ions, leading to the formation of transition metal-substituted POMs (TM-POMs)[40] (Fig. 1).

The incorporation of different metals into POMs alters their structural morphology by changing the bond distances between oxygen atoms and metals, with these distances varying based on the atomic radii of the metals. These structural modifications, in turn, affect the electronic distribution within the POMs, directly influencing their acid–base properties and redox activity.[41,42] Additionally, the introduction of transition metals can increase the number or variety of catalytic sites, thereby enhancing the overall catalytic performance and efficiency of POMs in various reactions.[25,43] Moreover, given the highly deterministic nature of their structures, POMs are ideal models for investigating metal oxide-anchored single-atom catalysts (SACs). This enables a comprehensive exploration of the coordination environment, electronic interactions, and the relationship between the structure and catalytic activity in SACs, often through theoretical computational studies.[23]

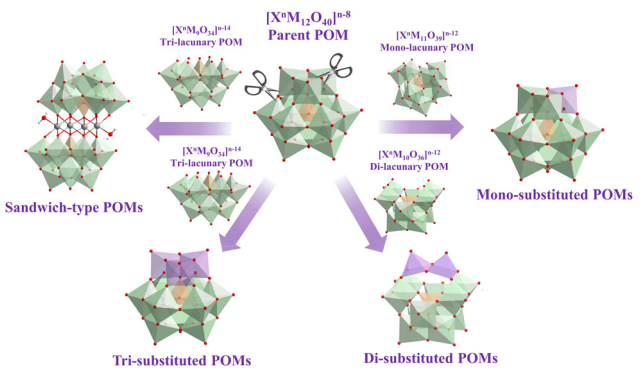

Fig. 1 Schematic illustration of the synthesis of transition metal substituted POM with lacunary POMs derived from parent POM. where X = P/Si; M = Mo/W and *n* = charge on X.

Additionally, the multiple lacunar building blocks of POMs facilitate the formation of transition metal clusters when using high-nuclear POMs.[44] Beginning with simple oxyoctahedra and their oligomers, POMs can self-assemble under specific conditions into multinuclear giant clusters with diverse shapes, such as sandwiches,[45] rings,[46] and wheels.[47] These clusters display novel properties that are not present in mononuclear POMs, thereby expanding the possibilities for further research and applications.

Furthermore, covalent modifications of POMs can be achieved by introducing functional groups such as photosensitive molecules, surfactants, and biomolecules. These modifications can enhance their photoresponsive, redox, acidic, hydrophilic, and hydrophobic properties.[48] By enriching the physicochemical characteristics of POMs, these functionalization create new opportunities for their application. The combined effects of organic and inorganic components can optimize the electronic structure and stability of POMs, thereby expanding their use in fields such as electrocatalysis, photocatalysis, molecular electronics, and nanomaterials.[49]

As previously discussed, POMs exhibit remarkable structural tunability, which can be precisely engineered by modulating factors such as elemental composition, anion type, valence states, and overall structure.[50,51] However, the practical application of POMs is often hindered by challenges related to their instability and tendency to agglomerate.[50,52]

Furthermore, POMs often have low specific surface areas, further reducing their catalytic reactivity.[53] To address these challenges, developing POM-based composites has emerged as a promising strategy to broaden their applicability. To facilitate broader applications across various fields, it is essential to incorporate additional functional properties into the substrate materials. These properties may include enhanced electrical conductivity for electrocatalysis.[54,55] (*e.g.*, carbon materials, metals, and conducting polymers) or improved light absorption and charge transport for photocatalysis.[56]

Recent studies have increasingly emphasized the synergistic effects between POMs and functional materials. As a result, composites based on POMs are being developed to allow these compounds to engage in catalytic processes across various fields. The following section discusses different strategies for synthesizing POM-based composites (Fig. 2).

(1) Supported POM-based composites: common materials used for this purpose include carbon-based materials (such as carbon nanotubes,[57] graphene,[58] and porous carbon[59]), mesoporous silica,[60] metal oxides,[61] and metals.[62] Several techniques are available for loading POMs onto these carriers, including impregnation, electrochemical deposition, sol–gel processes,

Open Access Article. Published on 28 February 2025. Downloaded on 2026-01-28 12:39:06 PM.
This article is licensed under a Creative Commons Attribution-NonCommercial 3.0 Unported Licence.

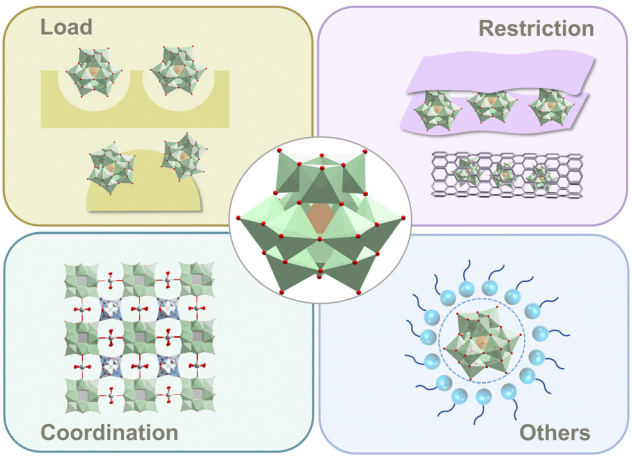

Fig. 2 Schematic illustration of four methods for synthesizing POM-based composites.

solvothermal synthesis, and co-precipitation.[63] These supported POM-based composites can be synthesized in a simple way, but there are often problems with the loading amount and dispersion degree.

(2) Restricted POM-based composites: the confinement strategy offers a promising approach for the stable immobilization of POMs within the pores of carriers. This prevents agglomeration and enhances the stability of the POMs. It also facilitates better dispersion and improves the electrical conductivity of the composite.

The synthesis of restricted POM-based composites starts with selecting the carrier material. Common restraint materials include one-dimensional tubular structures, two-dimensional layered materials, and three-dimensional porous materials.[52] Carbon nanotubes (CNTs) are a typical example of tubular carriers, where electrostatic interactions confine POMs within the CNTs, modulating their electronic properties and enhancing POM conductivity.[64,65] In layered materials, the large surface area facilitates a uniform distribution of POMs, minimizing aggregation and increasing the availability of active sites.[66] Three-dimensional porous materials, such as amphiphilic SiO_2@C nanorods,[67] organic porous materials like covalent organic frameworks (COFs),[68] and hybrid metal–organic frameworks (MOFs),[69] provide the stable pore structure that effectively prevents the loss of active components while ensuring that the active sites remain exposed. MOFs, in particular, are noteworthy for their ultra-high internal surface area, making them an ideal choice for confining POMs in catalytic applications.[50,70]

(3) POMOF materials: polyoxometalate-based metal–organic frameworks (POMOFs) are a unique class of materials where POMs are integrated through coordination with metal centers or organic ligands. These materials can be synthesized using two main approaches: solvothermal synthesis and stepwise synthesis.[71]

In solvothermal synthesis, metal salts, POMs (or their precursors), organic ligands, and solvents are made to react at high temperatures and pressures to yield highly crystalline POMOFs.[72,73] However, this technique is sensitive to reaction conditions, including the type and ratio of reactants, pH, temperature, and solvent choice, which may lead to variability in the results.[74,75]

The stepwise synthesis method involves two primary strategies: in the first strategy, metal ions or clusters react with POMs to generate modified POM derivatives, which can then serve as building blocks for further POMOF synthesis. The second strategy selects appropriate organic ligands to functionalize the POMs, allowing them to assemble with metal ions or clusters into a POMOF structure.[76–78] This approach provides greater control over the synthesis process and enables the design of POMOFs with tailored properties. The synthesis method of POMOF materials is rather complicated and demanding. However, the POMOF often has a definite structure, which is conducive to our further understanding of the catalytic mechanism.

3. POM molecular catalysts for the catalytic reduction of nitrogen oxide and its derivatives

3.1. Parent polyoxometalates

Polyoxometalates (POMs) offer significant advantages in catalytic applications due to their tunable acidic and redox properties, excellent thermal stability, structural diversity, and notable photoresponsivity.[79] Numerous studies have highlighted the impressive catalytic activity of these POMs, particularly in the reduction of nitrogen oxides (NO_x). For example, Yang and Chen[80] reported that small polar molecules, such as pyridine, alcohols, NO, and NH_3, can penetrate the bulk structure of POMs and interact with both the surface and the interior protons. These polar molecules primarily absorb by replacing the structural H_2O between the Keggin units of HPAs.[81] Among various POMs, the Keggin-type $H_3PW_{12}O_{40}$ has proven to be an effective NO_x adsorbent. The ability to adsorb significant amounts of polar NO and NO_2, along with its resistance to SO_2 poisoning, has made it a subject of extensive research. Notably, the adsorbed NO_x is reported to exist as NOH^+ and N_2O_3 rather than as nitrate in the bulk structure.[82] $H_3PW_{12}O_{40}$ demonstrates excellent performance in NO_x removal, with a rapid heating process that enables the decomposition of NO_x into N_2. At approximately 150 °C, NO is initially absorbed into the bulk of the heteropoly compound particles. Upon rapid heating to around 450 °C, decomposition takes place, resulting in the formation of N_2.[80]

By modulating the composition, topology, and pore structure of POMs, their structural parameters can be precisely controlled, allowing for customization specific to catalytic reactions. This customization enhances catalytic performance in targeted reactions.[83,84] By adjusting the type of coordinating atoms, several germanium-based Keggin-type POMs can be synthesized, including $H_4GeW_{12}O_{40}$ (HGeW), $H_5GeW_{11}VO_{40}$ (HGeWV), $H_5GeMo_{11}VO_{40}$ (HGeMoV) and $H_5GeW_9Mo_2VO_{40}$ (HGeWMoV). These compounds are considered promising candidates for NO_x adsorption and reduction.[85]

 This journal is © The Royal Society of Chemistry 2025

Open Access Article. Published on 28 February 2025. Downloaded on 2026-01-28 12:39:06 PM.
This article is licensed under a Creative Commons Attribution-NonCommercial 3.0 Unported Licence.

Besides the Keggin-type, Dawson-type HPAs are some of the most extensively studied. Dawson-type HPAs have a polyanion with an ellipsoidal shape, while the Keggin-type HPAs have a body-centered cubic structure with a spherical shape. Studies have shown that Dawson-type HPAs exhibit an active pseudo-liquid phase and can adsorb more polar molecules on their solid structure and surface than Keggin ones.[86] Due to its ultra-acidity and exceptional stability, Dawson-type HPAs demonstrate excellent catalytic activity in a variety of acid-catalyzed reactions.[87,88] Specifically, the Dawson-type $H_6P_2W_{18}O_{62}{\cdot}28H_2O$ (HP_2W) is an effective adsorbent for NO removal. HP_2W can achieve a maximum NO adsorption efficiency of 90% at 200 °C under mild conditions.[89]

POMs are considered polyspherical anions, and the electrostatic model (charge repulsion) explains the observed shift towards more negative reduction potentials as the total anionic charge of the POM increases.[90] Zhou *et al.*[91] investigated the influence of charge and redox potential in Keggin-type POMs on the electrochemical reduction of nitrite (NO_2^-) and nitrous acid (HNO_2) (Fig. 3). Differential electrochemical mass spectrometry (DEMS) analysis revealed that at pH 2 and 5, the first one-electron reduction wave of POMs (*e.g.*, $[PW_{12}O_{40}]^{3-}$, $[SiW_{12}O_{40}]^{4-}$, $[BW_{12}O_{40}]^{5-}$) exclusively produces nitric oxide (NO). However, when a two-electron reduction occurs, both NO and nitrous oxide (N_2O) are detected as products. The potential of the first reduction wave is strongly correlated with the charge of the POM, meaning that NO and/or N_2O are generated at lower overpotentials for $[PW_{12}O_{40}]^{3-}$ and $[SiW_{12}O_{40}]^{4-}$, compared to $[BW_{12}O_{40}]^{5-}$ and $[H_2W_{12}O_{40}]^{6-}$. Turnover frequency (TOF) was used to characterize and establish a hierarchy for these POMs. A clear trend was observed for TOF, as it depended on the redox potential of the POMs. Under the low pH of 2 and at lower overpotentials, the order of decreasing TOF is $[PW_{12}O_{40}]^{3-} > [SiW_{12}O_{40}]^{4-} > [BW_{12}O_{40}]^{5-}$. This order reverses at higher overpotentials. At pH 5 and with high overpotential, TOF values are about 70 times lower than the values at pH 2, likely due to a reduction in proton concentration and increased charge repulsion between the POM and NO_2^-.

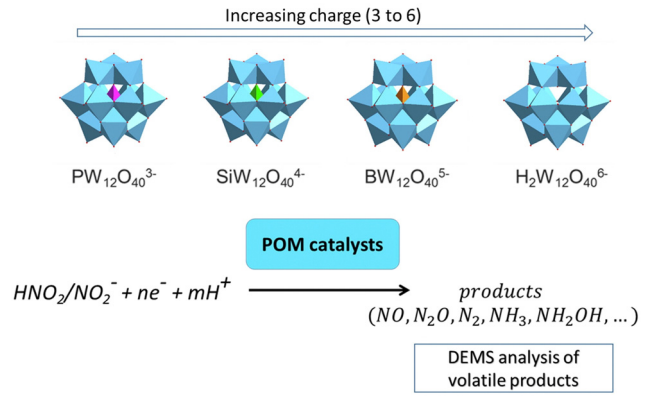

Fig. 3 Coordination polyhedral representation of all studied POMs. Oxygen atoms are depicted in red, blue polyhedra are formed by W atoms, and central atoms (tetrahedra) are depicted in specific color (P pink, Si green, B orange, H no color). POMs are used as catalysts free in solution for converting nitrous acid or nitrite to different products, and DEMS is used to identify volatile products. Adapted with permission.[91] Copyright 2021, Elsevier.

In addition to their impressive performance in reducing nitrogen oxides (NO_x), POMs have also shown significant potential in the hydrogenation of nitrobenzene.[92] The redox properties of POMs make them particularly appealing as inorganic molecular redox mediators in electro-organic transformations, especially for the indirect electro-reduction of nitrobenzene. In this indirect electrolysis process, the redox mediator acts as a bridge for electron transfer between the electrode and the substrate in the solution. Specifically, the mediator is oxidized at the anode surface; then, it diffuses into the solution, where it reduces the organic substrate. After this reduction, the mediator returns to the anode to be re-oxidized. This system allows the oxidized substrate to undergo subsequent chemical reactions in the solution, effectively decoupling the electron transfer from these reactions.[93] This decoupling mechanism not only prevents undesirable side reactions involving other functional groups but also enhances the selectivity of the nitrobenzene hydrogenation reaction. Furthermore, it helps avoid the accumulation of high-energy intermediates, which are common in direct electro-reduction processes, ensuring that the reaction proceeds efficiently.[94]

MacDonald *et al.*[95] were the first to report that electrochemically reduced POMs, specifically $H_4SiW_{12}O_{40}$ (SiW_{12}), can selectively hydrogenate a range of nitroarenes with other functional groups to their corresponding anilines (Fig. 4a). In a follow-up study,[94] they introduced another Keggin-type POM, $H_3PW_{12}O_{40}$ (PW_{12}), into the electrolyzer. This innovation effectively decouples the traditional direct electrochemical hydrogenation of nitrobenzene (Ph-NO_2) into a surface-homogeneous redox catalytic route (Fig. 4b). Rather than directly reducing nitrobenzene on the electrode surface, this method uses a soluble redox mediator ($H_3PW_{12}O_{40}$) as an electron and proton shuttle to selectively reduce the nitro groups in nitrobenzene derivatives (Fig. 4b). This straightforward approach is potentially more sustainable than conventional methods, as it eliminates the need for hydrogen gas, high temperatures, precious metal co-catalysts, and sacrificial reagents. Furthermore, the process operates in an aqueous solution at room temperature and pressure, utilizing electrons and protons derived from water. The mediator is recoverable and recyclable using well-established procedures and commonly available chemicals. The recycled mediator can also be electrochemically re-reduced and used for hydrogenation reactions without a significant decrease in performance compared to a fresh mediator. Given the scale and environmental impact of aniline production, this electrochemical route shows considerable promise for the development of more sustainable processes for producing these essential chemical feedstocks.

However, the specific mechanisms underlying redox mediator catalysis remain unclear, which hinders the screening and rational design of potential redox mediators. Building on these findings, our group[97] employed *in situ* electrochemical surface-enhanced Raman spectroscopy (EC-SERS) to investigate the

Open Access Article. Published on 28 February 2025. Downloaded on 2026-01-28 12:39:06 PM.
This article is licensed under a Creative Commons Attribution-NonCommercial 3.0 Unported Licence.

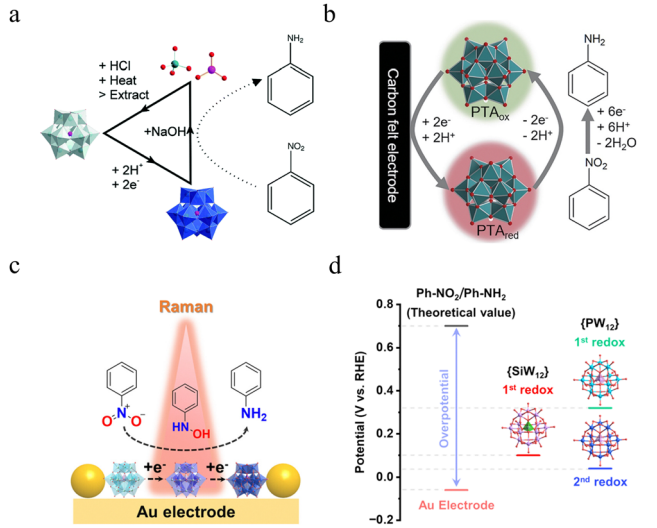

Fig. 4 (a) Schematic detailing the process of hydrogenating nitro-containing arene compounds and recycling the polyoxometalate. Adapted with permission.[95] Copyright 2018, Royal Society of Chemistry. (b) Illustration of the electrochemical, PTA-mediated, nitrobenzene to aniline reduction. Adapted with permission.[96] Copyright 2022, Elsevier. (c) Schematic illustration of EC-SERS analysis for $\{PW_{12}\}$-mediated hydrogenation of Ph-NO_2. (d) Comparison of the redox potentials of different reduced POMs and the hydrogenation potentials of Ph-NO_2 to Ph-NH_2. Adapted with permission.[97] Copyright 2024, American Chemical Society.

electrocatalytic reaction of nitrobenzene and its hydrogenation pathway in the presence of redox mediators under acidic conditions (Fig. 4c). The EC-SERS results confirmed the preferential adsorption and reduction of POMs as mediators on the electrode surface, showing strong interactions between the POMs and intermediates.

By comparing reactions catalyzed by different POM mediators, we found that the activation energy for reactions mediated by $1e^-$ reduced $\{PW_{12}\}$ (shortened as $1e^-\{PW_{12}\}$) was significantly higher than that for reactions mediated by $1e^-\{SiW_{12}\}$ and $2e^-\{PW_{12}\}$ mediators (Fig. 4d). This suggests that the redox potential differences among the POM mediators directly affect their electron-donating ability, which in turn influences hydrogenation conversion efficiency. Notably, using $\{PW_{12}\}$ as the redox mediator, the potential for hydrogenation of Ph-NO_2 to Ph-NH_2 was improved to 0.04 V *vs.* RHE with a high k_{app} of 0.0339 min^{-1}. These findings provide a valuable theoretical framework for a deeper understanding of the nitrobenzene hydrogenation reaction and the pivotal role of redox mediators, laying the groundwork for the development of more efficient redox mediators and advanced hydrogenation strategies.

3.2. Transition metal-substituted POMs

Transition metal-substituted polyoxometalates (TM-POMs), which consist of transition metal ions integrated into lacunary POMs frameworks, are not only structurally diverse but also play a pivotal role in various fields, including catalysis, materials science, and food chemistry.[98]

By modulating the electron density at the catalytic center, transition metals can substantially enhance the redox capacity of POMs while also improving their acidic properties, thereby boosting their catalytic activity.[39] Previous studies have shown that incorporating transition metals such as vanadium (V), copper (Cu), and iron (Fe) into the structural framework of POMs can significantly enhance their catalytic performance in nitrate reduction reactions.[99,100]

For instance, substituting vanadium into the framework of tungstic or molybdic-tungstic POMs increases the negative charge of the anion, which is expected to shift the stability of the saturated species to higher pH values. Moreover, studies on the electronic structure and catalytic behavior of vanadium-substituted POMs have revealed that introducing vanadium facilitates the reduction of NO and nitrite.[99] Similarly, incorporating transition metals such as copper and nickel (Ni) not only enhances the electrocatalytic activity of POMs but also significantly improves their long-term stability.[45] Furthermore, factors such as the number and position of substituents and the interactions between metal centers are crucial in determining the catalytic performance.[101,102] For example, in the α_2-$P_2W_{15}Mo_2Cu$ system,[100] the molybdenum (Mo) and copper (Cu) centers exhibit a notable synergistic effect. This synergy greatly enhances the electrocatalytic activity of POMs and substantially strengthens their electrochemical stability. Specifically, Cu significantly increases the molybdenum center's reduction potential, an effect absent in the copper-free system. Further atomic force microscopy (AFM) analysis confirmed the impact of Cu introduction on the surface morphology of POMs. The AFM images showed that Cu deposition induced changes in the surface morphology of POMs, suggesting that a synergistic effect exists between Mo and Cu centers at the morphological level.[103] Together, these synergistic effects contributed to the electrochemical performance and catalytic efficiency of the POMs.

In addition, the cumulative effect of copper plays a crucial role in enhancing the catalytic activity, particularly with respect to the number of substituents.[93] For example, it was reported that the dimeric pentacopper(II)-substituted tungstosilicate $[Cu_5(OH)_4(H_2O)_2(\alpha\text{-}SiW_9O_{33})_2]^{10-}$ catalyzes the reduction of nitrogen protoxide (N_2O), marking the first report of POM-catalyzed N_2O reduction.[104] In this and several other cases, both the nature and number of substituents work synergistically to influence the catalytic process. Focusing specifically on Cu-substituted POMs, comparisons between monosubstituted derivatives and sandwich-type complexes have highlighted the favorable impact of accumulating Cu centers within the same molecule, particularly for the electrocatalytic reduction of nitrate.[105,106] Similar observations have been made regarding Ni-multi-substituted POMs *versus* Ni^{2+}-monosubstituted POMs, and Fe^{3+}-sandwich-type POMs *versus* Fe^{3+}-monosubstituted POMs in various reaction processes.[107,108] A particularly striking example is the electrocatalytic behavior of the new Cu^{2+}-multi-substituted POM, $[Cu_{20}Cl(OH)_{24}(H_2O)_{12}(P_8W_{48}O_{184})]^{25-}$ ($Cu_{20}P_8W_{48}$), which contains twenty Cu atoms.[102] This finding further supports the notion that the accumulation of active Cu^{2+} centers within polyoxometalates is associated with enhanced catalytic properties, providing the added benefit of forming highly reduced species with the electrons accumulated

Open Access Article. Published on 28 February 2025. Downloaded on 2026-01-28 12:39:06 PM.
This article is licensed under a Creative Commons Attribution-NonCommercial 3.0 Unported Licence.

in the reduced W framework of the heteropolyanion. Furthermore, compared to the sandwich-type $Cu_4P_4W_{30}$ system, the accumulation of Cu^{2+} centers in the $Cu_{20}P_8W_{48}$ system causes a significant shift in the redox potential of the Cu and W centers, making it more conducive to the nitrate reduction reaction.[102]

Multi-lacunary polyoxometalates (POMs) serve as versatile building blocks due to their additional coordination sites, which enhance the modulation of electronic structures and facilitate the formation of high-nuclear transition metal clusters. Unlike monometallic acids, high-nuclear POM clusters can adjust both their electronic structures and geometric configurations over a broader range, resulting in a greater diversity of catalytic behaviors. Furthermore, an increase in cluster nuclearity can induce synergistic effects, further enhancing the catalytic performance.[44] For instance, Sun *et al.*[46] successfully synthesized a novel all-inorganic cyclic silver–polyoxometalate (Ag–POM) complex in a purely inorganic environment. This was achieved by precisely regulating the assembly process between the hollow ring $\{P_6W_{37}\}$ unit and the central silver cluster $\{Ag_6\}$. The resulting complex demonstrated outstanding photocatalytic activity in the reduction of nitrobenzene, achieving a remarkable conversion rate of 98.55% and a selectivity exceeding 99% within 2.5 hours, all while displaying excellent recyclability. (Fig. 5a). In another study, Tang *et al.*[109] synthesized a novel heteropolytungstate by coordinating four $\{Ru(C_6H_6)\}$ units with trivacant $\{TeW_9O_{33}\}$ clusters. Under visible light irradiation, it exhibited exceptional photocatalytic activity for the reduction of nitrobenzene, achieving a yield of 99.8%, with a turnover number (TON) of 330 and a turnover frequency (TOF) of 24 h^{-1}, thereby demonstrating its remarkable photocatalytic efficiency. (Fig. 5b). Additionally, Shi *et al.*[110] synthesized hexa-nuclear sandwich-type POMs ($Sb_8Mo_{18}O_6$) through an ionothermal method, representing the largest antimonomolybdate monomer. This complex displayed remarkable and sustainable catalytic activity in the reduction of nitrobenzene to aniline. The excellent catalytic performance was believed to arise from the synergistic interaction between the strong Lewis basic site Sb and the $[EMIm]^+$ cation, further emphasizing the significance of multifaceted synergistic mechanisms in facilitating efficient reactions.

The "bottom-up" molecular design strategy has made it possible to assemble POM structures, particularly in the construction of high-nuclear POM assemblies.[44] Under acidic conditions, the $\{P_2W_{12}\}$ building block easily undergoes self-assembly, forming a cyclic tetramer unit, $[H_7P_8W_{48}O_{184}]^{33-}$. This unit is characterized by its high structural stability and a large central cavity (approximately 10 Å in diameter), functioning as a well-defined, rigid molecular nano-reactor.[46,113,114] Additionally, the abundant coordination of oxygen sites within the cavity promotes interactions with metal cations, making it

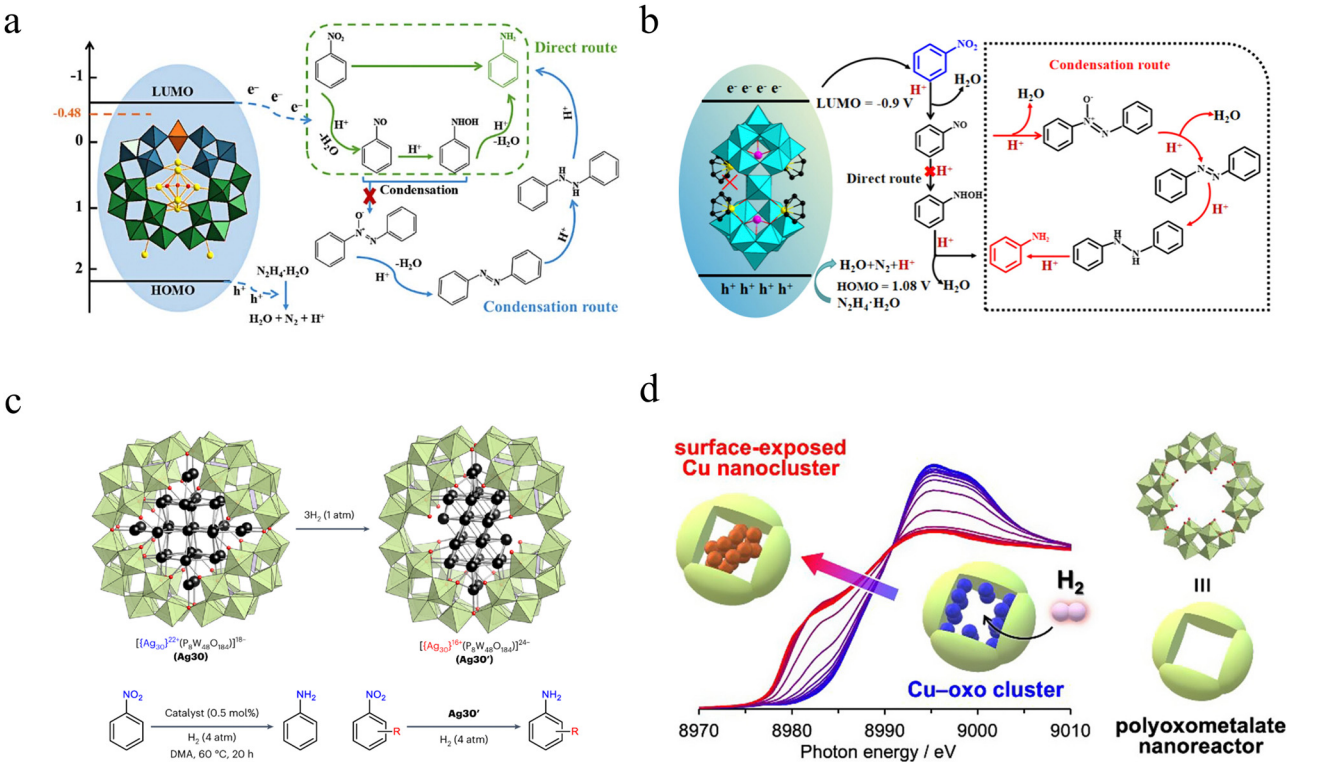

Fig. 5 (a) Proposed photoreduction reaction mechanism of $\{Ag_6\}$. Adapted with permission.[111] Copyright 2024, Royal Society of Chemistry. (b) The proposed mechanism of the photocatalytic NB conversion into AN of $\{Ru(C_6H_6)\}$-containing POM. Adapted with permission.[109] Copyright 2024, American Chemical Society. (c) Structure transformation and catalytic application of the $\{Ag_{30}\}$ nanocluster using H_2. Adapted with permission.[112] Copyright 2022, Springer Nature. (d) Synthesis of Cu nanoclusters through the solid-state reduction of Cu^{2+} incorporated within POMs. Reproduced with permission.[46] Copyright 2024, American Chemical Society.

Open Access Article. Published on 28 February 2025. Downloaded on 2026-01-28 12:39:06 PM.
This article is licensed under a Creative Commons Attribution-NonCommercial 3.0 Unported Licence.

an ideal support material for stabilizing metal clusters. This capability effectively prevents the leaching and aggregation of metal atoms, thereby improving both catalytic activity and stability.[46,115,116]

For example, Suzuki *et al.*[112] synthesized well-defined $\{Ag_{30}\}$ nanoclusters within the cavity of the cyclic POM $[P_8W_{48}O_{184}]^{40-}$. These nanoclusters exhibited exposed silver surfaces and interfaces with metal oxides. The synthesis process involved sequential reactions between P_8W_{48}, Ag^+ ions, and a reducing agent. The resulting silver nanoclusters demonstrated excellent catalytic performance in the selective reduction of nitrobenzene under mild reaction conditions. Crystallographic analysis revealed that the catalytic activity primarily arose from the interaction between the exposed surface of the silver nanoclusters and the metal–oxide interface, shedding light on the origins of the catalytic effect. This finding emphasizes the potential of using cyclic POM cavities to synthesize metal nanoclusters with accessible surfaces, promoting the exploration of their unique properties and applications, especially in conjunction with metal–oxide supports (Fig. 5c).

In a separate study, Suzuki *et al.*[46] conducted a solid-state reduction of an inorganic $\{P_8W_{48}\}$ framework containing a predetermined number of Cu^{2+} ions at 40 °C using H_2. This process successfully produced copper nanoclusters with exposed surfaces within the rigid and stable cyclic POM nanoreactor, featuring a defined number of Cu atoms. Furthermore, by alternating the gas atmosphere between H_2 and oxygen (O_2), the Cu nanoclusters underwent reversible redox transitions within the cavity. The hydrogen produced by these Cu nanoclusters effectively catalyzed the hydrogenation of various functional groups, such as alkenes, alkynes, carbonyls, and nitro groups, using H_2 as a reducing agent. Notably, the cyclic POM nanoreactor exhibited excellent durability during the H_2 reduction process, preventing the leaching and aggregation of copper atoms even after multiple redox cycles and catalytic reactions.[44]

3.3. POM molecular model catalysts

The structural properties of POM clusters make them highly effective ligands and carriers for constructing single-atom catalysts (SACs) with atomically precise structures. In these systems, both the coordination environment and the loading of active sites can be meticulously controlled. POM-SACs effectively bridge the gap between heterogeneous and homogeneous catalysis in complex hydrogenation reactions, facilitating the precise design of catalytic active centers at the molecular scale.[117] For example, in the Keggin-type anionic $[XM_{12}O_{40}]^{n-}$ system (where X can be B, Si, and P, and M typically refers to Mo or W), the metal centers present varying coordination environments, such as linear (coordination number CN = 2), trigonal (CN = 3), and tetragonal (CN = 4) sites.[23,118] These configurations closely resemble the active sites found in traditional SACs supported on metal oxides, allowing POMs to stabilize and efficiently generate metal sites. This significantly enhances the catalytic performance by providing stable, well-defined active sites and promoting reactions with greater efficiency.

A pioneering study by Yan's group has made significant advancements in this field. They synthesized a highly loaded Pt single-atom catalyst by impregnating phosphomolybdic acid (PMA) with Pt using a wet-impregnation method.[119] In this structure, each Pt atom is stabilized on a classical four-coordinate quasi square-planar geometry. Compared to conventional Pt/AC catalysts, the Pt-PMA/AC catalysts exhibit excellent performance in the hydrogenation of nitrobenzene, producing aniline as the sole product. This enhanced selectivity can be attributed to the unique adsorption and polarization effects of the Pt atoms on the PMA framework, which induce an electron out-flow. This underscores the distinct advantages of POMs in tuning catalyst selectivity and promoting highly specific reactions (Fig. 6b).

More importantly, the controlled hydrolysis properties of POMs allow for the selective removal of one or more metal–oxygen units, resulting in the formation of lacunary clusters. In these clusters, single-atom catalysts (SACs) can be integrated into the POM framework rather than being simply attached to its surface. These isolated binding sites create ''coordination islands'', which not only stabilize the SACs effectively but also provide diverse active sites for catalytic reactions.[23]

Previous studies have shown that POMs can effectively prevent the leaching and loss of metal centers, significantly enhancing the stability of catalysts. Additionally, the novel structure can introduce new catalytic effects and behaviors, optimizing reaction rates. For instance, Yan *et al.*[120] synthesized single-atom

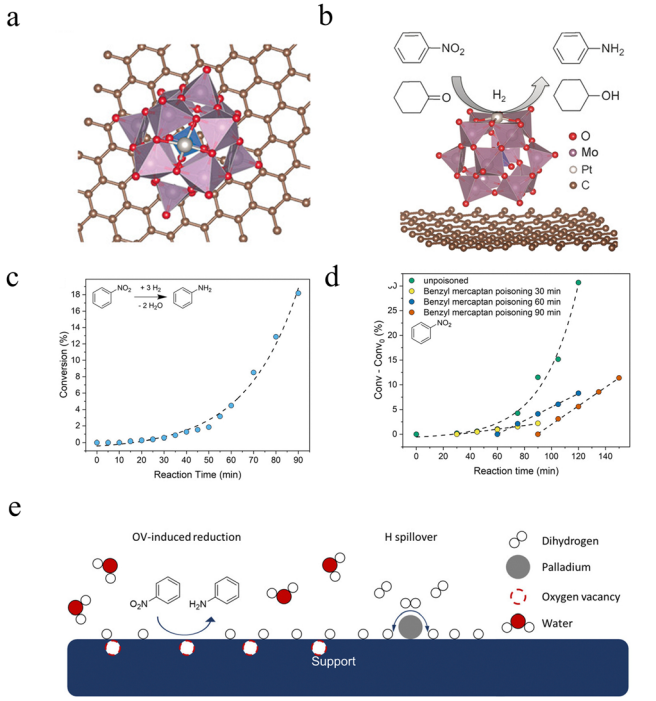

Fig. 6 (a) Top view and (b) side view of the most stable configuration of Pt_1 on PMA/graphene. Adapted with permission.[119] Copyright 2016, Wiley-VHC. (c) Conversion for the nitrobenzene (NB) hydrogenation during the hydrogen spillover. (d) Reaction kinetics for the hydrogenation of NB with the addition of 2 equivalents benzyl mercaptan after different reaction times. (e) Schematic depiction of the contribution of spilled over H to hydrogenation catalysis for NB. Adapted with permission.[120] Copyright 2022, Wiley-VHC.

This journal is © The Royal Society of Chemistry 2025

Open Access Article. Published on 28 February 2025. Downloaded on 2026-01-28 12:39:06 PM.
This article is licensed under a Creative Commons Attribution-NonCommercial 3.0 Unported Licence.

Pd-loaded model catalysts using soluble lacunary phosphomolybdic acid ($PMo_{11}O_{39}$) as support (Pd-SAC) and thoroughly analyzed their hydrogen spillover (H-spillover) behaviors in a homogeneous system. The findings reveal the kinetic and thermodynamic aspects of the H-spillover process (Fig. 6c) and clarify the intrinsic relationship between H-spillover and hydrogenation performance through kinetic tests and site poisoning experiments (Fig. 6d). The study indicates that the H-spillover effect is closely associated with the type of substrate functional group. Notably, during the hydrogenation of nitrobenzene, an enhancement in H-spillover significantly increases the reaction rate. This provides a theoretical basis for optimizing hydrogenation reactions (Fig. 6e).

Polyoxometalates serve as excellent molecular models, aiding in theoretical calculations and modeling. This enhances our understanding of the structure–activity relationship between the active sites and the catalytic activity of single-atom catalysts. Zhao *et al.*[121] investigated the catalytic mechanism of phosphomolybdic acid (PMA)-supported platinum (Pt) single-atom catalysts (Pt_1/Na_3PMA) in the hydrogenation of nitrobenzene (Ph-NO_2). Their study elucidates the mechanism of N–O bond cleavage during the reaction, demonstrating that the Pt single-atom catalytic site is central to the process. Meanwhile, the polyoxometalates function as "electron sponges," continuously donating and accepting electrons throughout the catalytic cycle. Notably, the POMs are crucial in facilitating N–O bond cleavage, highlighting their importance in the catalytic process. This discovery provides valuable insights into the mechanisms of POM-based catalysts in complex organic reactions. Furthermore, the study conducted a systematic comparison of the catalytic performance of various transition metals (*e.g.*, Pd, Ag, and Au) supported on Na_3PMA. The results reveal that Pd_1/Na_3PMA catalysts exhibit superior catalytic activity compared to other metal-based catalysts. This comparative analysis underscores the significant influence of metal selection on catalytic performance, offering a theoretical framework for optimizing POM-based catalysts in organic reactions (Fig. 7a).

In a related study,[122] transition metal-substituted Keggin-type POMs ($SiW_{11}Fe$) were used in the electrocatalytic reduction of nitrogen oxides (NO_x) for ammonia formation. This study revealed that the critical step in ammonia synthesis is the initial hydrogenation (*NO → *NHO), which has the lowest kinetic barrier (0.65 eV) and governs the overall reaction efficiency. A screening of catalysts substituted with various transition metals, including Ni^{2+}, Co^{2+}, Cu^{2+}, Pd^{2+}, Pt^{2+}, and Ag^{+}, demonstrated that Ni-substituted POM catalysts achieved optimal catalytic performance. The study further highlighted that the oxygen reduction ability and alkali strength of the transition metals were key factors influencing the hydrogenation process. These findings provide a valuable theoretical foundation for designing high-performance electrocatalysts for NO_x reduction (Fig. 7b).

3.4. Organic functionalization

POMs possess a multitude of modifiable sites for the incorporation of functional groups, which bestow a range of properties, including controllable hydrophilicity and tunable counter-cations.[123]

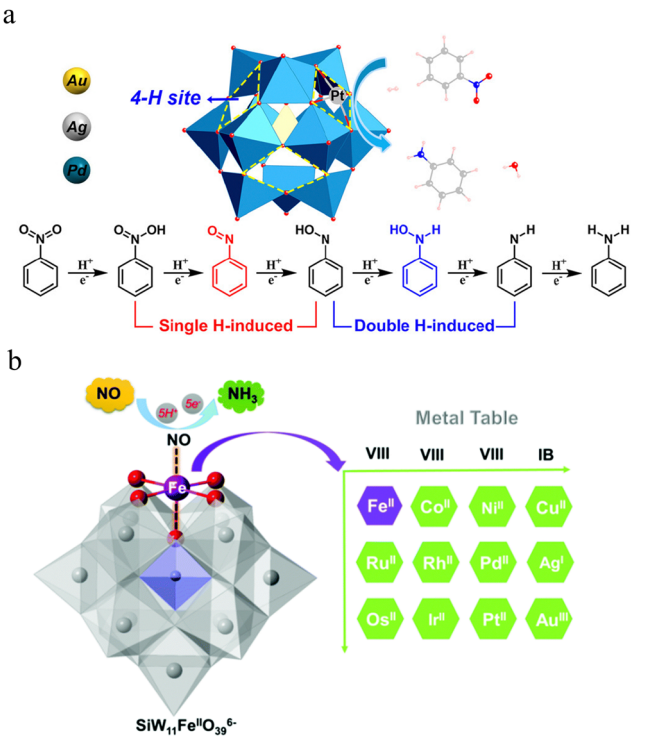

Fig. 7 (a) Proposed possible reaction pathways for the reduction of nitrobenzene into aniline. Adapted with permission.[121] Copyright 2024, American Chemical Society. (b) Polyhedral and ball-stick representation of the mono-Fe-substituted Keggin structure (left) applied in the NOER, and element table of potential substituting transition metals (right). The SiO_4 and WO_6 polyhedra are shown in light blue and grey, respectively. The Fe metal and its surrounding O atoms are shown as purple and red balls. Adapted with permission.[122] Copyright 2020, American Chemical Society.

This versatility facilitates enhanced modification potential through rational design. Typically, polymers,[124] organic molecules,[125] and other organic or inorganic clusters[126] can be grafted onto POMs to create building blocks with diverse compositions and shapes through organic synthesis strategies. Moreover, the properties of these POM-based building blocks can be fine-tuned by adjusting the composition of the POMs themselves, thus influencing their catalytic properties.[49]

Shima *et al.*[127] designed and synthesized an innovative lacunary polyoxometalate-based compound to serve as a heterogeneous catalyst. The catalyst was functionalized with lacunary Keggin-type POMs ($[PMo_{11}O_{39}]^{7-}$) *via* the use of 3-aminopropyltrimethoxysilane (APTS) and 2-pyridine carboxyaldehyde. Upon reaction with Cu^{2+} ions (Fig. 8a), the functionalized catalyst (LPMo-Cu) exhibited remarkable efficiency, achieving 100% conversion for the reduction of nitroaromatics, alongside excellent stability and recyclability (Fig. 8b). In a subsequent study, Shima *et al.*[48] prepared a heterogeneous nanocatalyst (POM-$PPPh_3$/L/Ni) by functionalizing $H_3PMo_{12}O_{40}$ with (3-bromopropyl)triphenylphosphonium bromide ($BPPPh_3Br$) through strong electrostatic interactions to prepare $[PMo_{12}O_{40}][PPPh_3]_3$ (referred to as POM-$PPPh_3$) (Fig. 8c). The final catalysts, produced by reacting polydentate Schiff base ligands and undergoing nickel cation metallization, showcased exceptional catalytic

Open Access Article. Published on 28 February 2025. Downloaded on 2026-01-28 12:39:06 PM.
This article is licensed under a Creative Commons Attribution-NonCommercial 3.0 Unported Licence.

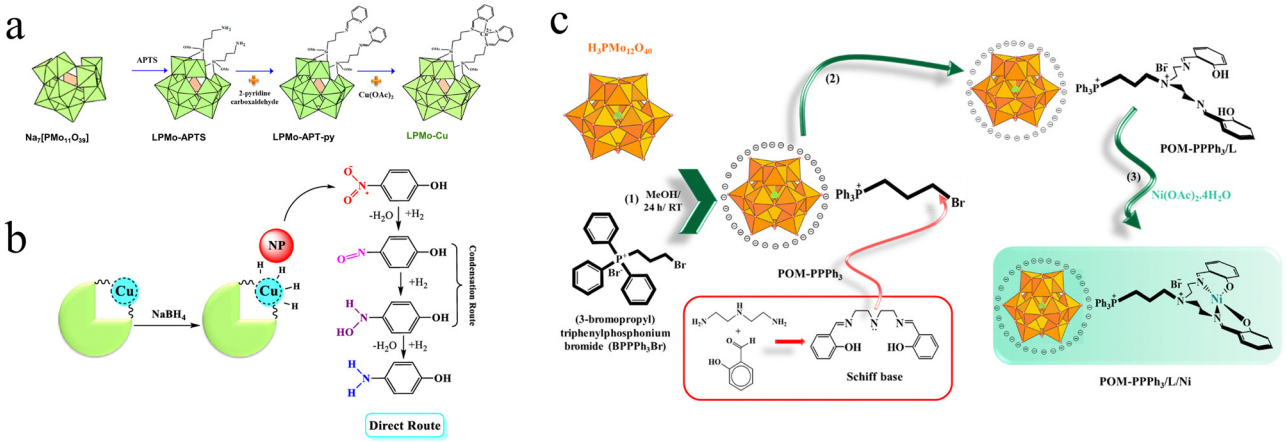

Fig. 8 (a) Schematic representation of the LPMo-Cu formation process and (b) proposed reaction path (direct path) for the reduction of the nitro group to the amino group. Adapted with permission.[127] Copyright 2023, American Chemical Society. (c) Proposed schematic of the route for the preparation of the POM-$PPPh_3$/L/Ni nanocatalyst. Adapted with permission.[48] Copyright 2024, Royal Society of Chemistry.

activity in the presence of $NaBH_4$. These catalysts accomplished efficient reduction of nitroaromatics within 10 minutes under aqueous conditions at ambient temperature, demonstrating excellent conversion efficiency.

4. POM-based composites for the catalytic reduction of nitrogen oxide and its derivatives

Polyoxometalates (POMs) are typically soluble in water and polar organic solvents. However, the high solubility in these solvents presents significant challenges, particularly in terms of recovery. Additionally, separating products in catalytic reactions can be problematic. In homogeneous catalysis, the catalytic activity of POMs may be hindered by self-aggregation, which increases costs and limits their industrial applicability.[79,128] Therefore, expanding the use of POMs from single crystalline materials to POM-based composites can enhance their utility in industry. For POM-based composite materials, several factors influence the catalytic performance. These include the inherent activity of the catalyst, the distribution and dispersion of active sites, the nature of the catalytic center, the specific surface area available for activity, and the catalytic synergies between the POMs and their support, *etc.*[71] Therefore, it is important to select an appropriate support and assembly structure, and to utilize non-covalent interactions (*e.g.*, electrostatic interactions, hydrogen bonding, π–π stacking) and covalent interactions (*e.g.*, ligand substitution) in the design and synthesis of functionalized POM-based composites to optimize catalytic performance. We classify the methods for assembling POM-based composites into three main approaches: loading, confinement, and coordination interactions.

4.1. Supported POM-based composites

Polyoxometalates exhibit remarkable redox properties. However, their limited surface area significantly restricts their applications in catalytic systems.[50] To overcome this limitation, loading POMs onto functional substrates allows for their effective utilization in a wide range of catalytic processes. Various methods can be used to immobilize POMs on different substrates. The selection of functional materials is usually customized for the specific catalytic process being targeted.

In catalytic reduction systems, utilizing different solid carriers or substrates to support POMs can significantly enhance their surface area, reaction sites, catalytic activity, electron transfer efficiency, and stability. For instance, Bahram Yadollahi *et al.*[129] synthesized POM@g-C_3N_4 composites by protonating g-C_3N_4 and utilizing impregnation and electrostatic self-assembly interactions to incorporate the POM anion. This method effectively increased the catalytic surface area, electron transfer capability, and redox potential of the composites. As a result, these composites demonstrated excellent catalytic performance in reducing various nitroaromatic compounds in aqueous systems.

Conductive substrates (such as nickel foam, graphene, carbon cloth, *etc.*),[17] along with traditional photocatalytic carriers (SiO_2, TiO_2, *etc.*),[130] serve as effective media for enhancing the performance of POMs in photocatalytic and electrocatalytic systems. In electrocatalytic reactions, loading POMs onto conductive materials with a high specific surface area can significantly improve catalyst conductivity and reduce interfacial resistance between the catalyst and the carrier. The increased surface area also exposes more active sites.[131] Lee *et al.*[132] demonstrated the loading of Fe-POM onto Cu foams using the drop-casting method with an ionomer (Fig. 9a). The resulting Fe-POM/Cu electrocatalysts facilitate the generation of hydrogen radicals in the Volmer reaction. The high binding affinity of Cu metal for NO_3^- and the synergistic action between Cu and Fe-POM lead to efficient and selective reduction of nitrate to ammonia, achieving a faradaic efficiency of up to 97.09%. The combination of POMs and conductive polymer complexes offers another approach to enhance the electrocatalytic performance. Zhang *et al.*[20] successfully created a novel conductive composite membrane that contains Keggin-type

Open Access Article. Published on 28 February 2025. Downloaded on 2026-01-28 12:39:06 PM.
This article is licensed under a Creative Commons Attribution-NonCommercial 3.0 Unported Licence.

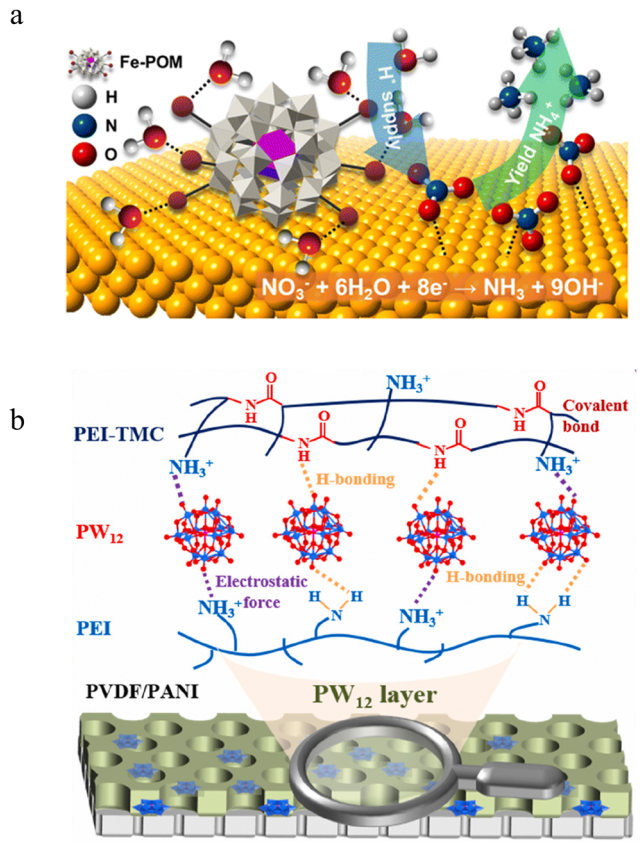

Fig. 9 (a) Schematic illustration of electrocatalyst nitrate hydroreduction to ammonia on the Fe-POM/Cu. Adapted with permission.[132] Copyright 2024, Royal Society of Chemistry. (b) The assembly structure of conductive composite membranes doped with POMs for nitrite removal. Adapted with permission.[20] Copyright 2024, Elsevier.

polyoxometalates utilizing layer-by-layer self-assembly and interfacial polymerization on a conductive substrate (Fig. 9b). They employed electrostatic binding between negatively charged $[PW_{12}O_{40}]^{3-}$ (PW_{12}) and positively charged polyethyleneimine (PEI) to uniformly integrate POMs into the selective layer, forming a highly stable conductive composite film. Under an electric field, this membrane exhibited excellent electrical responsiveness, achieving a removal rate of NO_2 of 81%. In photocatalytic systems, materials like TiO_2 are advantageous due to their non-toxicity, stability, high catalytic activity, and strong oxidative ability. However, their quantum efficiency is often limited by the rapid recombination of photogenerated electron–hole pairs. The strong electron-acceptor properties of POMs can alleviate these limitations. By loading POMs onto TiO_2, the recombination rate of electron–hole pairs can be reduced, thereby enhancing photocatalytic performance.[133] For example, Wang *et al.*[133] synthesized a composite photocatalyst (SiW_9/TiO_2/Cu) *via* the sol–gel method, which exhibited significantly improved photocatalytic activity for nitrate reduction under UV light compared to pure TiO_2. This enhancement was attributed to the extended lifetime of electron–hole pairs, facilitated by the POMs and Cu in combination with TiO_2, which synergistically increased the photocatalytic activity.

Furthermore, POMs can serve not only as active sites for catalysis but also as terminal agents or stabilizers, providing added stability to nanoparticles. Their inherent stability under acidic, alkaline, thermal, and oxidative conditions makes them excellent ligands for use in harsh reaction environments. Yamazoe *et al.*[134] synthesized Nb_6–Au/Al_2O_3 catalysts by modifying $[Nb_6O_{19}]^{8-}$ clusters with gold nanoparticles (Au NPs) supported on Al_2O_3. This yields bifunctional catalysts that possess both reduction and base properties (Fig. 10a). The Nb_6–Au/Al_2O_3 catalysts demonstrated high catalytic selectivity, achieving a selectivity of over 99% for *p*-aminophenol, and proved highly effective in the selective reduction of nitroaromatics. Similarly, Ke *et al.*[135] developed a $H_3PW_{12}O_{40}$ (HPW) modified Pt_1/CeO_2 catalyst through impregnation (Fig. 10b). In this system, the electronic interactions mediated by POMs facilitated the selective catalytic reduction of nitric oxide. The process involves electron transfer from CeO_2 to HPW, followed by electron transfer from the Pt atoms to the electron-deficient ceria. This sequential transfer leads to an enhanced positive charge on the Pt atoms, ultimately accelerating the degradation of NO. Moreover, Ayati *et al.*[136] created an Au NPs/HPW/TiO_2 nanotube (NT) photocatalyst to promote the degradation of nitrobenzene. In this system, HPW acts as an "electron scavenger," transferring photogenerated electrons and thereby inhibiting the rapid electron–hole recombination of TiO_2 nanotubes. Additionally, due to the photoactivity of HPW molecules and their exceptional electron transfer capabilities, the HPW bridging layer between TiO_2 and Au NPs provides an extra driving force for charge transfer between them.

4.2. Restricted POM-based composites

In heterogeneous catalytic reactions, the catalytic process usually takes place on the surface of a solid catalyst. For reactants to reach the active sites, they must first diffuse through the catalytic boundary layer. Both the adsorption of the reactants and the desorption of the products are critical factors that influence catalytic efficiency. The pore structure not only minimizes the aggregation of POM species, preventing the loss of active components, but also enhances the exposure of active sites. However, composites based on POMs that rely solely on depositing POMs onto support often struggle with uneven dispersion. Additionally, the interactions between POMs and the support may not sufficiently stabilize the anchoring of POMs, which can lead to the leaching of the active components. This leaching significantly undermines the cycling stability of heterogeneous phase catalysts.

The confinement strategy is an effective approach for immobilizing polyoxometalates, typically synthesized through simple methods that enable the stable incorporation of guest species (*e.g.*, clusters, nanoparticles, molecules, *etc.*) within the pristine pores or channels of the host material.[52] This strategy effectively prevents the loss of active components while promoting the homogeneous dispersion of the guest species. Such composites not only maintain the individual advantages of each component but also benefit from synergistic interactions that enhance performance and widen application possibilities.

Open Access Article. Published on 28 February 2025. Downloaded on 2026-01-28 12:39:06 PM.
This article is licensed under a Creative Commons Attribution-NonCommercial 3.0 Unported Licence.

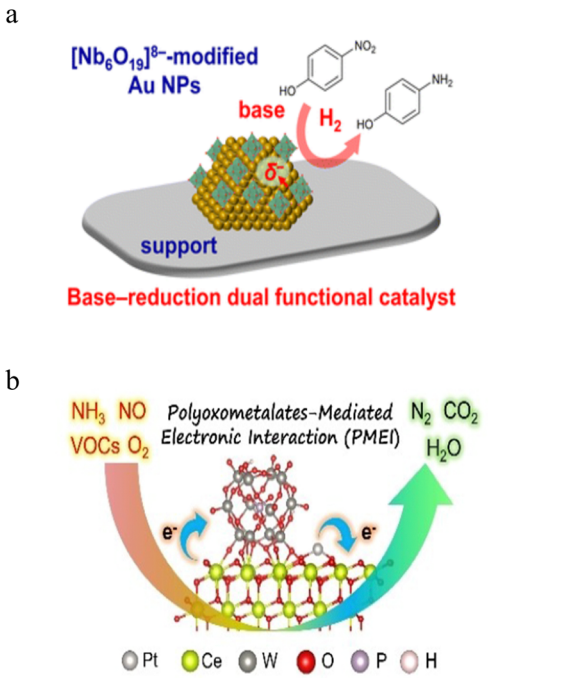

Fig. 10 (a) Schematic diagram of the Nb_6–Au/Al_2O_3 catalyst for catalytic reduction of nitroaromatic hydrocarbons. Adapted with permission.[134] Copyright 2022, Royal Society of Chemistry. (b) Polyoxometalates-mediated electron interaction promotes the selective catalysis of Pt_1/CeO_2 for nitric oxide. Adapted with permission.[135] Copyright 2024, Wiley-VHC.

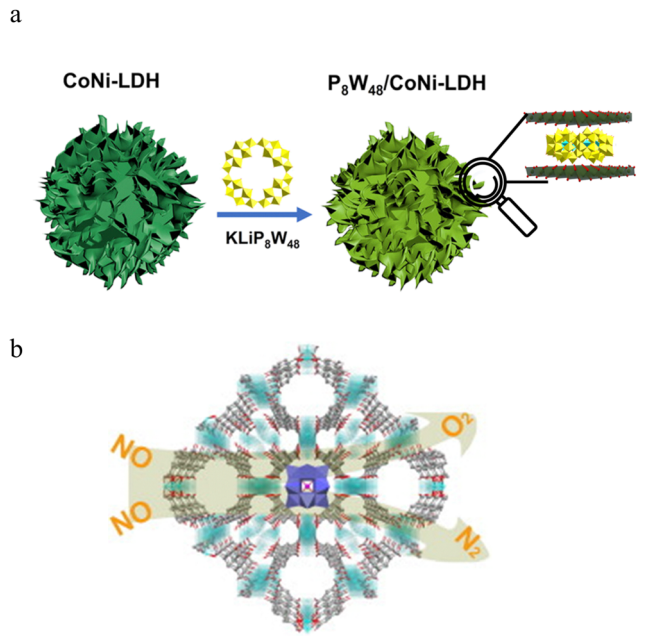

Fig. 11 (a) Illustration of the structure diagram of limited catalyst P_8W_{48}/CoNi-LDH. Adapted with permission.[137] Copyright 2024, American Chemical Society. (b) Schematic diagram of NO decomposition of the composite based on metal–organic frameworks and polyoxometalates. Adapted with permission.[138] Copyright 2012, Elsevier.

Layered double hydroxides (LDHs) are a representative class of materials that consist of positively charged metal hydroxide layers.[75] POMs, as anionic clusters, can be confined within the layers of LDH, resulting in the formation of POM@LDH composites. These composites offer several advantages: they reduce the tendency of POMs to agglomerate and leach, facilitate the immobilization of POMs, and expose more active sites. Zhang *et al.*[137] synthesized P_8W_{48}/CoNi-LDH nanocomposites (Fig. 11a), which demonstrated excellent catalytic activity and cycling stability in the conversion of nitrite to ammonia (NH_3). The CoNi-LDHs, characterized by their high specific surface area, promote the physical enrichment of NO_2^- on this composite. Meanwhile, the Lewis acid sites of P_8W_{48} further enhance the adsorption of NO_2^-, acting as an electron transfer carrier to accelerate reaction kinetics. This catalyst exhibits superior NO_2^- reduction reaction (NO_2RR) performance, achieving a faradaic efficiency of 97.0% at −1.3 V *versus* AgCl/Ag.

Metal–organic frameworks (MOFs) are a promising class of porous crystalline materials characterized by their open framework structure, permanent porosity, high specific surface area, and tunable hydrophilic–hydrophobic channels.[139,140] To further enhance their performance, researchers incorporate POMs into MOFs using various methods such as encapsulation, impregnation, ion exchange, substitution, and covalent grafting. The combination of POMs, known for their redox properties, with the porosity of MOFs enables efficient multiphase catalysis. POM@MOF materials offer several advantages, including the provision of suitable hydrophobic and hydrophilic microenvironments and optimized mass transfer channels. These features enhance the interaction between active sites and substrates, promote the diffusion of reactants and products, and ultimately improve catalytic efficiency. For example, Yao *et al.*[141] synthesized two POM@MOF materials, namely $[Cd(btbu)_2(H_2O)_2(PMo_{12}O_{40})]$ (CUST-636) and $[Cd(btbu)_2(H_2O)(SiW_{12}O_{40})_{0.5}]$ (CUST-638), using the hydrothermal method (Fig. 11b). Their studies showed that these materials exhibited excellent catalytic performance in nitrite reduction. Additionally, Ma *et al.* presented a POM-based porous composite, $H_4[(Cu_4Cl)_3(BTC)_8]_2[SiW_{12}O_{40}]\cdot(C_4H_{12}N)_6\cdot 3H_2O$ (NENU-15, where BTC = 1,3,5-benzenetricarboxylate), to remove nitric oxide (NO). In this open structure, the exposed Cu^{2+} sites and the guest POMs play essential roles in the adsorption of NO. The introduction of POMs significantly enhanced the material's thermal stability and facilitated the decomposition of NO, demonstrating the synergistic effects of these components in catalytic processes.

4.3. POMOF materials

Ligand interactions also provide an effective strategy for the immobilization of polyoxometalates. Polyoxometalate-based metal–organic frameworks (POMOFs) are a class of extended structures that combine the advantageous properties of both POMs and metal–organic frameworks (MOFs). Due to their numerous potential coordination sites, POMs can interact in various ways with their precursors and metal–organic components, resulting in the formation of POMOFs. POMOFs are typically characterized by excellent thermal stability and can be

 This journal is © The Royal Society of Chemistry 2025

Open Access Article. Published on 28 February 2025. Downloaded on 2026-01-28 12:39:06 PM.
This article is licensed under a Creative Commons Attribution-NonCommercial 3.0 Unported Licence.

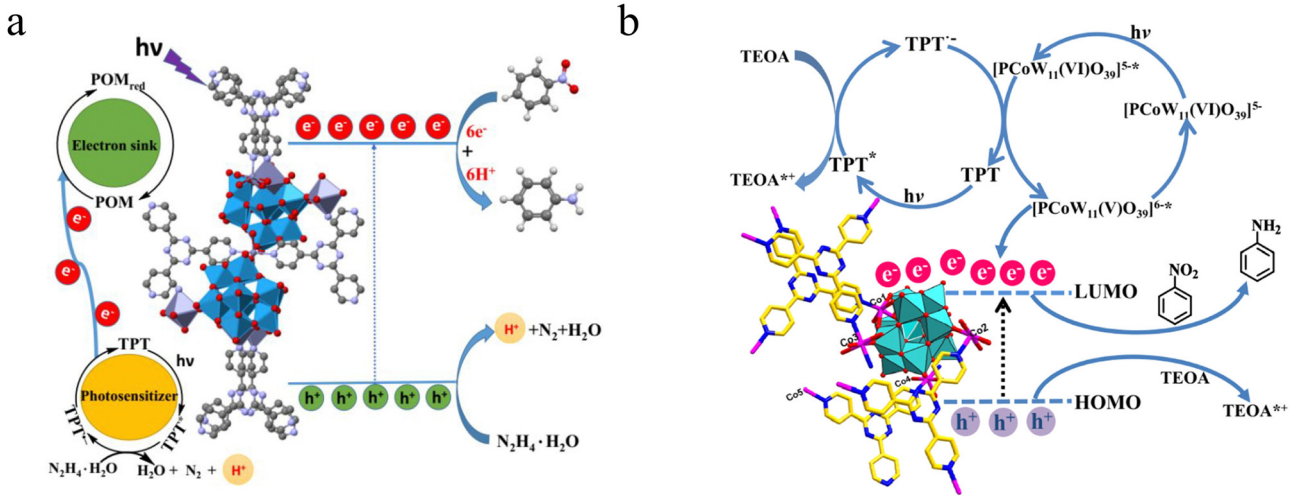

Fig. 12 (a) Photocatalytic diagram of the {CoW-TPT} for reduction of nitrobenzene. Adapted with permission.[142] Copyright 2022, American Chemical Society. (b) Photocatalytic diagram of the {ZnW-TPT} for reduction of nitroarenes. Adapted with permission.[143] Copyright 2022, American Chemical Society.

easily recycled multiple times, making them highly suitable for use as heterogeneous catalysts. They generally possess precise chemical compositions and structures, which facilitate the study and exploration of catalytic mechanisms. The organic fragments within POMOFs can be customized through organic synthesis to suit the requirements of different catalytic reactions. This includes selective synthesis of hydrophilic or lipophilic materials according to specific catalytic systems.

An example of a promising photosensitizer for constructing photocatalysts is 2,4,6-tris(4-pyridyl)-1,3,5-triazine (TPT), which features a nanoscale conjugated surface, strong light absorption properties, and exceptional electrical conductivity. Importantly, TPT can be irradiated with light to generate solid-state triplet double radicals. In their research, Chen *et al.*[142] successfully synthesized a new metal–organic framework, CoW-TPT, based on POMs by incorporating Co(II)-substituted keggin-type POMs, specifically $[PW_{11}CoO_{39}]^{5-}$.(Fig. 12a). The charge transfer between $[PW_{11}CoO_{39}]^{5-}$ and TPT enhances the reduction of nitrobenzene. The direct ligand binding between $[PW_{11}CoO_{39}]^{5-}$ and the TPT ligand, along with structural interactions, creates an effective pathway for charge transfer. This increases the likelihood of forming critical TPT-radical anions, leading to an impressive reduction efficiency of 94.71% for nitrobenzene using triethanolamine (TEOA) as the reducing agent. Additionally, Jiao *et al.*[143] synthesized a complex identified as $\{[HZn(TPT)SiW_{11}O_{39})][Zn(TPT)(H_2O)_3][Zn(H_2O)_4][Zn_{0.5}(TPT)(H_2O)]\}\cdot 4H_2O$, referred to as {ZnW-TPT} (Fig. 12b). In this structure, the POM acts as an electron trap to prevent the recombination of photogenerated electron holes during the multi-electron transfer process. The direct coordination between $[SiZnW_{11}O_{39}]^{6-}$ and the TPT ligand, along with interactions between TPT molecules, contributes to the separation and migration of photogenerated carriers. This enhances the photocatalytic activity for nitrobenzene hydrogenation in the {ZnW-TPT} structure.

5. Conclusion and perspectives

Polyoxometalates (POMs) are a unique class of metal–oxygen clusters characterized by their adjustable structures, exceptional redox properties, and high stability, making them excellent candidates for catalytic applications. Recent research has highlighted their potential in reducing nitrogen oxides (NO_x) by efficiently converting them into valuable nitrogen compounds, such as ammonia. This conversion offers a promising approach to restoring the natural nitrogen cycle and reducing environmental pollution. This review provided an overview of the application of POMs in the catalytic reduction of nitrogen oxide and its derivatives, including nitroaromatics and nitrogen oxides. The catalytic performance of POMs has been significantly enhanced through various modification strategies, such as transition metal doping, organo-functionalization, and the combination of POMs with other functionalized materials. These modifications improve the performance of POM-based catalysts in both homogeneous and heterogeneous catalysis while enhancing their selectivity and efficiency in processes like nitrogen oxide reduction and nitroaromatic hydrogenation.

However, despite these advancements, challenges regarding the stability, durability, and selectivity of POM-based catalysts in practical applications still exist. Future research should focus on several key areas:

(1) In-depth application of *in situ* characterization techniques: enabling *in situ* characterization techniques for real-time monitoring of dynamic changes during catalytic reactions allows for the precise identification of active sites and reaction pathways. However, current *in situ* methods face limitations, such as the complexity of equipment and challenges in data processing. Future research should focus on developing innovative *in situ* characterization methods, such as integrating time-resolved techniques to capture transient intermediate states or employing high-resolution imaging techniques to observe dynamic changes on the catalyst surface. Such advancements

Open Access Article. Published on 28 February 2025. Downloaded on 2026-01-28 12:39:06 PM. This article is licensed under a Creative Commons Attribution-NonCommercial 3.0 Unported Licence.

would provide more detailed reaction kinetics and mechanistic information. Furthermore, the integration of machine learning and artificial intelligence into *in situ* analysis platforms could enable real-time monitoring of reaction dynamics and automated data analysis, significantly enhancing research efficiency and accelerating the identification of key reaction mechanisms and optimal conditions.

(2) Innovation in customized structural design: by tailoring the structural composition of polyoxometalates and employing hybridization strategies with functional materials, such as carbon materials and metal–organic frameworks (MOFs), researchers can design catalysts with tailored activity and selectivity. In-depth investigations of structure–activity relationships, supported by computational chemistry methods like density functional theory (DFT), provide a theoretical foundation for the rational design of customized catalysts. Additionally, advanced computational approaches, including machine learning and quantum mechanical simulations, offer deeper insights into the electronic structure, active sites, and reaction mechanisms of POMs, providing robust guidance for the development of high-performance catalysts.

(3) Interdisciplinary integration of green catalysis and sustainable development: POMs demonstrate excellent biological activity and photocatalytic performance, with their reversible redox properties making them ideal redox couples that can bridge various systems.

For instance, POMs can facilitate the integration of photovoltaic systems with bioelectrochemical platforms and other green technologies, potentially leading to the development of more efficient and sustainable catalytic systems. Moreover, recent advancements in electrochemical synthesis have opened promising avenues for addressing energy and environmental challenges. The coupling of the electrochemical NO_x reduction reaction (NO_xRR) with organic carbon sources has provided new insights into the removal of NO_x pollutants and their conversion into valuable chemicals, such as amino acids, amides, urea, and other high-value products. This innovative approach not only addresses environmental concerns but also creates new opportunities for sustainable chemical production.

(4) Advancement in industrialization and practical applications: although POMs have demonstrated exceptional catalytic performance in laboratory settings, their stability, durability, and cost-effectiveness under industrial conditions still need further validation. Future efforts should focus on developing efficient, cost-effective synthetic methods to enable the large-scale production of POM-based catalysts, paving the way for their industrial application. In addition, improving the long-term stability and reusability of these catalysts through structural optimization will be critical for sustaining their performance over extended reaction cycles. Testing POM-based catalysts in simulated industrial environments will be essential for evaluating their applicability and reliability in complex reaction systems.

In summary, while POMs exhibit significant potential as catalysts in reactions such as the reduction of nitrogen oxide and its derivatives, their widespread adoption in practical applications still faces numerous challenges. However, with a deeper understanding of their structures, properties, and reaction mechanisms, POM-based catalysts are poised to play an increasingly vital role in environmental protection, energy storage, and chemical synthesis.

Author contributions

Yuan Jiang: resources, investigation, writing – original draft and writing – review and editing. Chun-Jun Chen: investigation, writing – original draft and writing – review and editing. Ke Li: formal analysis, investigation, and writing. Li-Ping Cui: writing – review & editing. Jia-Jia Chen: discussion, supervision, and writing – review & editing.

Data availability

No new data were created or analysed during this study.

Conflicts of interest

There are no conflicts to declare.

Acknowledgements

We acknowledge financial support from the National Key Research and Development Program (2021YFA1502300), the National Natural Science Foundation of China (NSFC, 22393901, 22021001, 22272143, and 22441030), the Fundamental Research Funds for the Central Universities (20720220009), the Fujian Provincial Natural Science Foundation of China (2024J01213135) and the Innovation Laboratory for Sciences and Technologies of Energy Materials of Fujian Province (IKKEM, RD2023020801). K. Li also acknowledges the support from the fellowship of China Postdoctoral Science Foundation (2024M761765).

References

1 K. A. Emhoff, A. M. H. Salem, L. Balaraman, D. M. Kingery and W. C. Boyd, *Results Chem.*, 2020, **2**, 100016.
2 D. Torres, S. Pérez-Rodríguez, L. Cesari, C. Castel, E. Favre, V. Fierro and A. Celzard, *Carbon*, 2021, **183**, 12–33.
3 X. Ren, L. Tang, J. Wang, E. Almatrafi, H. Feng, X. Tang, J. Yu, Y. Yang, X. Li, C. Zhou, Z. Zeng and G. Zeng, *Water Res.*, 2021, **201**, 2.
4 F. Liu, W. Chen, T. Wang, J. Zhang, D. Yang, Y. Dai, G. Liu, J. Zhou, S. Wang and X. Guan, *Angew. Chem., Int. Ed.*, 2025, **64**, e202415438.
5 X. Yan, L. Chen, H. Song, Z. Gao, H. Wei, W. Ren and W. Wang, *New J. Chem.*, 2021, **45**, 18268–18276.
6 G. Liu, C. Chen and J. Chen, *J. Phys. Chem. C*, 2023, **127**, 4375–4386.
7 D. E. Canfield, A. N. Glazer and P. G. Falkowski, *Science*, 2010, **330**, 192–196.
8 J. Long, S. Chen, Y. Zhang, C. Guo, X. Fu, D. Deng and J. Xiao, *Angew. Chem., Int. Ed.*, 2020, **59**, 9711–9718.
9 L. Collado, A. H. Pizarro, M. Barawi, M. García-Tecedor, M. Liras and V. A. De La Peña O'Shea, *Chem. Soc. Rev.*, 2024, **53**, 11334–11389.
10 Q. Zhu, P. Dong, J. Yu, Z. Wang, T. Wang, S. Qiao, J. Liu, S. Geng, Y. Zheng, P. Cheng, M. J. Zaworotko, Z. Zhang and Y. Chen, *Nat. Commun.*, 2025, **16**, 992.

 This journal is © The Royal Society of Chemistry 2025

Open Access Article. Published on 28 February 2025. Downloaded on 2026-01-28 12:39:06 PM. This article is licensed under a Creative Commons Attribution-NonCommercial 3.0 Unported Licence.

11 P. H. Van Langevelde, I. Katsounaros and M. T. M. Koper, *Joule*, 2021, **5**, 290–294.
12 Y. Xiong, Y. Wang, J. Zhou, F. Liu, F. Hao and Z. Fan, *Adv. Mater.*, 2024, **36**, 2304021.
13 J. John, D. R. MacFarlane and A. N. Simonov, *Nat. Catal.*, 2023, **6**, 1125–1130.
14 J.-Y. Fang, Q.-Z. Zheng, Y.-Y. Lou, K.-M. Zhao, S.-N. Hu, G. Li, O. Akdim, X.-Y. Huang and S.-G. Sun, *Nat. Commun.*, 2022, **13**, 7899.
15 D. Feng, L. Zhou, T. J. White, A. K. Cheetham, T. Ma and F. Wei, *Nano-Micro Lett.*, 2023, **15**, 203.
16 A. V. Anyushin, A. Kondinski and T. N. Parac-Vogt, *Chem. Soc. Rev.*, 2020, **49**, 382–432.
17 Z. Zeb, Y. Huang, L. Chen, W. Zhou, M. Liao, Y. Jiang, H. Li, L. Wang, L. Wang, H. Wang, T. Wei, D. Zang, Z. Fan and Y. Wei, *Coord. Chem. Rev.*, 2023, **482**, 215058.
18 W. Guan, G. Wang, B. Li and L. Wu, *Coord. Chem. Rev.*, 2023, **481**, 215039.
19 M. R. Horn, A. Singh, S. Alomari, S. Goberna-Ferrón, R. Benages-Vilau, N. Chodankar, N. Motta, K. (Ken) Ostrikov, J. MacLeod, P. Sonar, P. Gomez-Romero and D. Dubal, *Energy Environ. Sci.*, 2021, **14**, 1652–1700.
20 M.-M. Zhang, A.-K. Li, M.-J. Tang, Q.-Y. He, Y.-H. Peng, R.-J. Fan, S.-P. Sun and X.-L. Cao, *J. Membr. Sci.*, 2024, **699**, 122668.
21 H. Li, Z. Yuan, W. Chen, M. Yang, Y. Sun, S. Zhang, P. Ma, J. Wang and J. Niu, *J. Mater. Chem. A*, 2023, **11**, 10813–10822.
22 F.-Y. Yu, Z.-L. Lang, Y.-J. Zhou, K. Feng, H.-Q. Tan, J. Zhong, S.-T. Lee, Z.-H. Kang and Y.-G. Li, *ACS Energy Lett.*, 2021, **6**, 4055–4062.
23 R. Liu and C. Streb, *Adv. Energy Mater.*, 2021, **11**, 2101120.
24 Y.-F. Liu, C.-W. Hu and G.-P. Yang, *Chin. Chem. Lett.*, 2023, **34**, 108097.
25 S. D. Mürtz, J. Raabe, M. J. Poller, R. Palkovits, J. Albert and N. Kurig, *ChemCatChem*, 2024, **16**, e202301632.
26 F. Boussema, R. Haddad, Y. Ghandour, M. S. Belkhiria, M. Holzinger, A. Maaref and S. Cosnier, *Electrochim. Acta*, 2016, **222**, 402–408.
27 X. Zeng, Y. Jing, S. Gao, W. Zhang, Y. Zhang, H. Liu, C. Liang, C. Ji, Y. Rao, J. Wu, B. Wang, Y. Yao and S. Yang, *Nat. Commun.*, 2023, **14**, 7414.
28 A. Ebrahimi, L. Krivosudský, A. Cherevan and D. Eder, *Coord. Chem. Rev.*, 2024, **508**, 215764.
29 C. Dey, *J. Cluster Sci.*, 2022, **33**, 1839–1856.
30 Y. Liu, X. Wu, Z. Li, J. Zhang, S.-X. Liu, S. Liu, L. Gu, L. R. Zheng, J. Li, D. Wang and Y. Li, *Nat. Commun.*, 2021, **12**, 4205.
31 K. M. P. Wheelhouse, R. L. Webster and G. L. Beutner, *Org. Process Res. Dev.*, 2023, **27**, 1157–1159.
32 C. Zhu, L. Xu, Y. Liu, J. Liu, J. Wang, H. Sun, Y.-Q. Lan and C. Wang, *Nat. Commun.*, 2024, **15**, 4213.
33 W. Ahmad, N. Ahmad, K. Wang, S. Aftab, Y. Hou, Z. Wan, B. Yan, Z. Pan, H. Gao, C. Peung, Y. Junke, C. Liang, Z. Lu, W. Yan and M. Ling, *Adv. Sci.*, 2024, **11**, 2304120.
34 Q. Liu and X. Wang, *Matter*, 2020, **2**, 816–841.
35 M. Hutin, M. H. Rosnes, D.-L. Long and L. Cronin, *Comprehensive Inorganic Chemistry II*, Elsevier, 2013, pp. 241–269.
36 I. V. Kozhevnikov, *Chem. Rev.*, 1998, **98**, 171–198.
37 *Polyoxometalate Molecular Science*, ed. J. J. Borrás-Almenar, E. Coronado, A. Müller and M. Pope, Springer, Netherlands, Dordrecht, 2003.
38 G. Yang, Y. Liu and Y. Wei, *Coord. Chem. Rev.*, 2024, **521**, 216172.
39 A. Patel, N. Narkhede, S. Singh and S. Pathan, *Catal. Rev.*, 2016, **58**, 337–370.
40 Z. Wang, X. Xin, M. Zhang, Z. Li, H. Lv and G.-Y. Yang, *Sci. China: Chem.*, 2022, **65**, 1515–1525.
41 J.-C. Raabe, T. Esser, F. Jameel, M. Stein, J. Albert and M. J. Poller, *Inorg. Chem. Front.*, 2023, **10**, 4854–4868.
42 O. Tomita, H. Naito, A. Nakada, M. Higashi and R. Abe, *Sustainable Energy Fuels*, 2022, **6**, 664–673.
43 J. C. Ye, J. J. Chen, R. M. Yuan, D. R. Deng, M. S. Zheng, L. Cronin and Q. F. Dong, *J. Am. Chem. Soc.*, 2018, **140**, 3134–3138.
44 J.-C. Liu, J.-W. Zhao, C. Streb and Y.-F. Song, *Coord. Chem. Rev.*, 2022, **471**, 214734.
45 I. M. Mbomekalle, P. Mialane, A. Dolbecq, J. Marrot, F. Sécheresse, P. Berthet, B. Keita and L. Nadjo, *Eur. J. Inorg. Chem.*, 2009, 5194–5204.
46 Y. Koizumi, K. Yonesato, S. Kikkawa, S. Yamazoe, K. Yamaguchi and K. Suzuki, *J. Am. Chem. Soc.*, 2024, **146**, 14610–14619.
47 K. Li, S. Zhang, K.-L. Zhu, L.-P. Cui, L. Yang and J.-J. Chen, *J. Am. Chem. Soc.*, 2023, **145**, 24889–24896.
48 S. Aghajani and M. Mohammadikish, *Dalton Trans.*, 2024, **53**, 10644–10654.
49 J.-X. Liu, X.-B. Zhang, Y.-L. Li, S.-L. Huang and G.-Y. Yang, *Coord. Chem. Rev.*, 2020, **414**, 213260.
50 J.-J. Ye and C.-D. Wu, *Dalton Trans.*, 2016, **45**, 10101–10112.
51 S. Zhang, R. Liu, C. Streb and G. Zhang, *Polyoxometalates*, 2023, **2**, 9140037.
52 L. Guo, L. He, Q. Zhuang, B. Li, C. Wang, Y. Lv, J. Chu and Y. Song, *Small*, 2023, **19**, 2207315.
53 L. Yu, Q. Liu, S. Ding, J. Yu, S. Peng, J. Zhang, C. Jiang and G. Yang, *Appl. Surf. Sci.*, 2022, **602**, 154095.
54 R. Zhang and C. Yang, *J. Mater. Chem.*, 2008, **18**, 2691.
55 Y. Chen, F. Li, S. Li, L. Zhang and M. Sun, *Inorg. Chem. Commun.*, 2022, **135**, 109084.
56 X. Chen, H. Wu, X. Shi and L. Wu, *Nanoscale*, 2023, **15**, 9242–9255.
57 F. M. Toma, A. Sartorel, M. Iurlo, M. Carraro, P. Parisse, C. Maccato, S. Rapino, B. R. Gonzalez, H. Amenitsch, T. Da Ros, L. Casalis, A. Goldoni, M. Marcaccio, G. Scorrano, G. Scoles, F. Paolucci, M. Prato and M. Bonchio, *Nat. Chem.*, 2010, **2**, 826–831.
58 J. Lei, X.-X. Fan, T. Liu, P. Xu, Q. Hou, K. Li, R.-M. Yuan, M.-S. Zheng, Q.-F. Dong and J.-J. Chen, *Nat. Commun.*, 2022, **13**, 202.
59 R. He, K. Xue, J. Wang, Y. Yan, Y. Peng, T. Yang, Y. Hu and W. Wang, *Chemosphere*, 2020, **259**, 127465.
60 J.-Q. Wu, L. Ma, Z.-Z. Li, X. Li, S.-W. Li, C. Li, R.-X. Li and J.-S. Zhao, *Fuel*, 2024, **371**, 131902.
61 N. Shi, Y. Ding, N. Li, F. Wen and D. Liu, *J. Environ. Chem. Eng.*, 2023, **11**, 110558.
62 W. Luo, J. Hu, H. Diao, B. Schwarz, C. Streb and Y. Song, *Angew. Chem., Int. Ed.*, 2017, **56**, 4941–4944.
63 A. Khodadadi Dizaji, H. R. Mortaheb and B. Mokhtarani, *Mater. Chem. Phys.*, 2017, **199**, 424–434.
64 J. W. Jordan, G. A. Lowe, R. L. McSweeney, C. T. Stoppiello, R. W. Lodge, S. T. Skowron, J. Biskupek, G. A. Rance, U. Kaiser, D. A. Walsh, G. N. Newton and A. N. Khlobystov, *Adv. Mater.*, 2019, **31**, 1904182.
65 J. Sloan, G. Matthewman, C. Dyer-Smith, A.-Y. Sung, Z. Liu, K. Suenaga, A. I. Kirkland and E. Flahaut, *ACS Nano*, 2008, **2**, 966–976.
66 S. Omwoma, W. Chen, R. Tsunashima and Y.-F. Song, *Coord. Chem. Rev.*, 2014, **258–259**, 58–71.
67 H. Liu, Z. Li, J. Dong, D. Liu, C. Liu, Y. Chi and C. Hu, *Nanoscale*, 2020, **12**, 16586–16595.
68 Y. Zhang, D.-H. Yang, S. Qiao and B.-H. Han, *Langmuir*, 2021, **37**, 10330–10339.
69 F. Zhang, Y. Jin, J. Shi, Y. Zhong, W. Zhu and M. S. El-Shall, *Chem. Eng. J.*, 2015, **269**, 236–244.
70 C. T. Buru and O. K. Farha, *ACS Appl. Mater. Interfaces*, 2020, **12**, 5345–5360.
71 S. Zhang, F. Ou, S. Ning and P. Cheng, *Inorg. Chem. Front.*, 2021, **8**, 1865–1899.
72 J. Niu, S. Zhang, H. Chen, J. Zhao, P. Ma and J. Wang, *Cryst. Growth Des.*, 2011, **11**, 3769–3777.
73 D. Hagrman, P. J. Hagrman and J. Zubieta, *Angew. Chem., Int. Ed.*, 1999, **38**, 3165–3168.
74 D.-Y. Du, J.-S. Qin, S.-L. Li, Z.-M. Su and Y.-Q. Lan, *Chem. Soc. Rev.*, 2014, **43**, 4615–4632.
75 X.-X. Li, D. Zhao and S.-T. Zheng, *Coord. Chem. Rev.*, 2019, **397**, 220–240.
76 X. Li, Y. Wang, R. Wang, C. Cui, C. Tian and G. Yang, *Angew. Chem., Int. Ed.*, 2016, **55**, 6462–6466.
77 A. Dolbecq, C. Mellot-Draznieks, P. Mialane, J. Marrot, G. Férey and F. Sécheresse, *Eur. J. Inorg. Chem.*, 2005, 3009–3018.
78 L. Vilà-Nadal and L. Cronin, *Nat. Rev. Mater.*, 2017, **2**, 17054.
79 S.-S. Wang and G.-Y. Yang, *Chem. Rev.*, 2015, **115**, 4893–4962.
80 R. T. Yang and N. Chen, *Ind. Eng. Chem. Res.*, 1994, **33**, 825–831.
81 A. M. Herring and R. L. McCormick, *J. Phys. Chem. B*, 1998, **102**, 3175–3184.
82 R. Belanger and J. Moffat, *Appl. Catal., B*, 1997, **13**, 167–173.
83 H. Sampei, H. Akiyama, K. Saegusa, M. Yamaguchi, S. Ogo, H. Nakai, T. Ueda and Y. Sekine, *Dalton Trans.*, 2024, **53**, 8576–8583.

Open Access Article. Published on 28 February 2025. Downloaded on 2026-01-28 12:39:06 PM. This article is licensed under a Creative Commons Attribution-NonCommercial 3.0 Unported Licence.

84 I.-M. Mbomekallé, X. López, J. M. Poblet, F. Sécheresse, B. Keita and L. Nadjo, *Inorg. Chem.*, 2010, **49**, 7001–7006.
85 R. Wang, X. Zhang and Z. Ren, *J. Hazard. Mater.*, 2021, **402**, 123494.
86 M. Misono, *Chem. Commun.*, 2001, 1141–1152.
87 L. E. Briand, G. T. Baronetti and H. J. Thomas, *ChemInform*, 2004, **35**, 18248.
88 R. Tayebee, M. M. Amini, H. Rostamian and A. Aliakbari, *Dalton Trans.*, 2014, **43**, 1550–1563.
89 X. Zhang, R. Wang, H. Zhu and Y. Chen, *Chem. Eng. J.*, 2020, **400**, 125880.
90 L. M. Mbomekalle, X. López, J. M. Poblet, F. Sécheresse, B. Keita and L. Nadjo, *Inorg. Chem.*, 2010, **49**, 7001–7006.
91 Y. Zhou, F. Bihl, A. Bonnefont, C. Boudon, L. Ruhlmann and V. Badets, *J. Catal.*, 2022, **405**, 212–223.
92 A. D. Stergiou, D. H. Broadhurst and M. D. Symes, *ACS Org. Inorg. Au*, 2023, **3**, 51–58.
93 B. Keita and L. Nadjo, *J. Mol. Catal. A:Chem.*, 2007, **262**, 190–215.
94 A. D. Stergiou and M. D. Symes, *Cell Rep. Phys. Sci.*, 2022, **3**, 100914.
95 L. MacDonald, B. Rausch, M. D. Symes and L. Cronin, *Chem. Commun.*, 2018, **54**, 1093–1096.
96 S. R. Waldvogel and C. Streb, *Chem*, 2022, **8**, 2071–2073.
97 G.-F. Liu, S. Zhang, C.-J. Chen, S.-M. Xing, X.-Y. Zhang, Y.-J. Zhang, D.-Y. Wu, J.-F. Li, B. Ren and J.-J. Chen, *Chem. Mater.*, 2024, **36**(18), 8825.
98 D.-Q. Qian, Y.-D. Lin, H.-P. Xiao, B. Wu, X.-X. Li and S.-T. Zheng, *Polyoxometalates*, 2024, **3**, 9140040.
99 B. Keita, R. Contant, P. Mialane, F. Secheresse, P. Deoliveira and L. Nadjo, *Electrochem. Commun.*, 2006, **8**, 767–772.
100 B. Keita, E. Abdeljalil, L. Nadjo, B. Avisse, R. Contant, J. Canny and M. Richet, *Electrochem. Commun.*, 2000, **2**, 145–149.
101 U. Kortz, S. Nellutla, A. C. Stowe, N. S. Dalal, U. Rauwald, W. Danquah and D. Ravot, *Inorg. Chem.*, 2004, **43**, 2308–2317.
102 D. Jabbour, B. Keita, L. Nadjo, U. Kortz and S. Mal, *Electrochem. Commun.*, 2005, **7**, 841–847.
103 B. Keita, E. Abdeljalil, L. Nadjo, R. Contant and R. Belghiche, *Langmuir*, 2006, **22**, 10416–10425.
104 S. Nellutla, J. van Tol, N. S. Dalal, L.-H. Bi, U. Kortz, B. Keita, L. Nadjo, G. A. Khitrov and A. G. Marshall, *Inorg. Chem.*, 2005, **44**, 9795–9806.
105 B. Keita, I.-M. Mbomekalle and L. Nadjo, *Electrochem. Commun.*, 2003, **5**, 830–837.
106 B. Keita, I. Martyr Mbomekalle, L. Nadjo and R. Contant, *Electrochem. Commun.*, 2001, **3**, 267–273.
107 L.-H. Bi, U. Kortz, S. Nellutla, A. C. Stowe, J. van Tol, N. S. Dalal, B. Keita and L. Nadjo, *Inorg. Chem.*, 2005, **44**, 896–903.
108 I. M. Mbomekalle, B. Keita, L. Nadjo, P. Berthet, K. I. Hardcastle, C. L. Hill and T. M. Anderson, *Inorg. Chem.*, 2003, **42**, 1163–1169.
109 W. Tang, Y. Liu, Y. Jin, Y. Wang, W. Shi, P. Ma, J. Niu and J. Wang, *Inorg. Chem.*, 2024, **63**, 6260–6267.
110 S.-K. Shi, X. Li, H. Guo, Y. Fan, H. Li, D.-B. Dang and Y. Bai, *Inorg. Chem.*, 2020, **59**, 11213–11217.
111 Y. Sun, S. Zhang, M. Cai, P. Ma, J. Niu and J. Wang, *J. Mater. Chem. A*, 2024, **12**, 29580–29587.
112 K. Yonesato, D. Yanai, S. Yamazoe, D. Yokogawa, T. Kikuchi, K. Yamaguchi and K. Suzuki, *Nat. Chem.*, 2023, **15**, 940–947.
113 Q. Zhao, Y. Zeng, Z. Jiang, Z. Huang, D. Long, L. Cronin and W. Xuan, *Angew. Chem.*, 2024, e202421132.
114 J. Lin, N. Li, S. Yang, M. Jia, J. Liu, X.-M. Li, L. An, Q. Tian, L.-Z. Dong and Y.-Q. Lan, *J. Am. Chem. Soc.*, 2020, **142**, 13982–13988.
115 L. Qiao, M. Song, A. Geng and S. Yao, *Chin. Chem. Lett.*, 2019, **30**, 1273–1276.
116 R. Ge, X.-X. Li and S.-T. Zheng, *Coord. Chem. Rev.*, 2021, **435**, 213787.
117 Y. Ma, C. Chen, Y. Jiang, X. Wei, Y. Liu, H. Liao, H. Wang, S. Dai, P. An and Z. Hou, *ACS Catal.*, 2023, **13**, 10295–10308.
118 S. He, Q. Liu and X. Wang, *J. Mater. Chem. A*, 2022, **10**, 5758–5770.
119 B. Zhang, H. Asakura, J. Zhang, J. Zhang, S. De and N. Yan, *Angew. Chem., Int. Ed.*, 2016, **55**, 8319–8323.
120 M. J. Hülsey, V. Fung, X. Hou, J. Wu and N. Yan, *Angew. Chem., Int. Ed.*, 2022, **61**, e202208237.
121 C. Zhao, S. Wang, L. Yan and Z. Su, *Inorg. Chem.*, 2024, **63**, 1784–1792.
122 Z. Lang, J. Miao, H. Tan, Z. Su, Y. Li and Z. Zheng, *Inorg. Chem. Front.*, 2020, **7**, 4507–4516.
123 D. Li, Z. Liu, J. Song, H. Li, B. Zhang, P. Yin, Z. N. Zheng, J. E. Roberts, M. Tsige, C. L. Hill and T. Liu, *Angew. Chem., Int. Ed.*, 2017, **56**, 3294–3298.
124 S.-J. Yu, Y.-K. Han and W. Wang, *Polymer*, 2019, **162**, 73–79.
125 D. E. Salazar Marcano, S. Lentink, M. A. Moussawi and T. N. Parac-Vogt, *Inorg. Chem.*, 2021, **60**, 10215–10226.
126 J. Luo, K. Chen, P. Yin, T. Li, G. Wan, J. Zhang, S. Ye, X. Bi, Y. Pang, Y. Wei and T. Liu, *Angew. Chem., Int. Ed.*, 2018, **57**, 4067–4072.
127 S. Aghajani, M. Mohammadikish and M. Khalaji-Verjani, *Langmuir*, 2023, **39**, 8484–8493.
128 J. Zhong, J. Pérez-Ramírez and N. Yan, *Green Chem.*, 2021, **23**, 18–36.
129 N. Aramesh and B. Yadollahi, *Mater. Chem. Phys.*, 2023, **296**, 127308.
130 A. Di, J. Schmitt, M. A. Da Silva, K. M. Z. Hossain, N. Mahmoudi, R. J. Errington and K. J. Edler, *Nanoscale*, 2020, **12**, 22245–22257.
131 Y. Zhang, M. Luo, Y. Yang, Y. Li and S. Guo, *ACS Energy Lett.*, 2019, **4**, 1672–1680.
132 H. Lee, K.-H. Kim, R. R. Rao, D. G. Park, W. H. Choi, J. H. Choi, D. W. Kim, D. H. Jung, I. E. L. Stephens, J. R. Durrant and J. K. Kang, *Mater. Horiz.*, 2024, **11**, 4115–4122.
133 L. Wang, W. Fu, Y. Zhuge, J. Wang, F. Yao, W. Zhong and X. Ge, *Chemosphere*, 2021, **278**, 130298.
134 S. Kikkawa, S. Fukuda, J. Hirayama, N. Shirai, R. Takahata, K. Suzuki, K. Yamaguchi, T. Teranishi and S. Yamazoe, *Chem. Commun.*, 2022, **58**, 9018–9021.
135 T. Lan, R. Yalavarthi, Y. Shen, M. Gao, F. Wang, Q. Hu, P. Hu, M. Beladi-Mousavi, X. Chen, X. Hu, H. Yang, E. Cortés and D. Zhang, *Angew. Chem., Int. Ed.*, 2025, **64**, e202415786.
136 A. Ayati, B. Tanhaei, F. F. Bamoharram, A. Ahmadpour, P. Maydannik and M. Sillanpää, *Sep. Purif. Technol.*, 2016, **171**, 62–68.
137 L.-N. Zhang, G.-A. Jia, C. Ma, M.-Q. Jia, T.-S. Li, L.-B. Ni and G.-W. Diao, *Inorg. Chem.*, 2024, **63**, 6787–6797.
138 F.-J. Ma, S.-X. Liu, G.-J. Ren, D.-D. Liang and S. Sha, *Inorg. Chem. Commun.*, 2012, **22**, 174–177.
139 Y. Liu, C. Tang, M. Cheng, M. Chen, S. Chen, L. Lei, Y. Chen, H. Yi, Y. Fu and L. Li, *ACS Catal.*, 2021, **11**, 13374–13396.
140 J. Sun, S. Abednatanzi, P. Van Der Voort, Y.-Y. Liu and K. Leus, *Catalysts*, 2020, **10**, 578.
141 J. Yao, J. Sun, X. Li, Y. Lin, Y. Zhao, X. Chen, M. Li, Z. Wang and Z.-M. Su, *J. Mol. Struct.*, 2025, **1319**, 139485.
142 C. Si, F. Liu, X. Yan, J. Xu, G. Niu and Q. Han, *Inorg. Chem.*, 2022, **61**, 5335–5342.
143 J. Jiao, H. Sun, C. Si, J. Xu, T. Zhang and Q. Han, *ACS Appl. Mater. Interfaces*, 2022, **14**, 16386–16393.

 This journal is © The Royal Society of Chemistry 2025